Surgical Skills and Ergonomics Evaluation for Laparoscopic Surgery Training

SURGICAL SKILLS AND ERGONOMICS EVALUATION FOR LAPAROSCOPIC SURGERY TRAINING

BY

THU ZAR KYAW, B.Eng.

A THESIS

SUBMITTED TO THE DEPARTMENT OF ELECTRICAL & COMPUTER ENGINEERING

AND THE SCHOOL OF GRADUATE STUDIES

OF MCMASTER UNIVERSITY

IN PARTIAL FULFILMENT OF THE REQUIREMENTS

FOR THE DEGREE OF

MASTER OF APPLIED SCIENCE

Master of Applied Science (2013) McMaster University

(Electrical & Computer Engineering) Hamilton, Ontario, Canada

TITLE:	Surgical Skills and Ergonomics Evaluation for Laparoscopic Surgery Training
AUTHOR:	Thu Zar Kyaw B.Eng., (Electrical Engineering) McMaster University, Hamilton,Ontario, Canada
SUPERVISOR:	Dr. Jim Reilly and Dr. Alexandru Patriciu
NUMBER OF PAGES:	xv, 100

To my parents, sister, brother, and *all who have shared their knowledge as well as skills.*

Abstract

Training and ergonomics evaluation for laparoscopic surgery is an important tool for the assessment of trainees. Timely and objective assessment helps surgeons improve hand dexterity and movement precision, and perform surgery in an ergonomic manner. Traditionally, skill is evaluated by expert surgeons observing trainees, but this approach is both expensive and subjective. The approach proposed by this research employs an Ascension 3DGuidance trakSTAR system that captures the positions and orientations of hand and laparoscopic tool trajectories. Recorded trajectories are automatically analysed to extract meaningful feedback for training evaluation using statistical and machine learning methods.

The data are acquired while a subject performs a standardized task such as peg transfer or suturing. The system records laproscopic instrument positions, hand, forearms, elbows trajectories, as well as wrist angles. We propose several metrics that attempt to objectively quantify the skill level or ergonomics of the procedure. The metrics for surgical skills are based on surgical instrument tip trajectories, whereas the ergonomics metric uses wrist angles. These metrics have been developed using statistical and machine learning methods.

The metrics have been experimentally evaluated by using a population of seven first year postgraduate urology residents, one general surgery resident, and eight fourth year postgraduate urology residents and fellows. The machine learning approach discriminated correctly in 73% of cases between experts and novices. The machine learning approach applied to ergonomics data correctly discriminates between experts and novices in 88% of the cases for the peg transfer task and 75% for the suturing task. We also propose a method to derive a competency-based score using either statistical or machine learning derived metrics.

Initial experimental data show that the proposed methods discriminate between the skills and ergonomics of expert and novice surgeons. The proposed system can be a valuable tool for research and training evaluation in laparoscopic surgery.

Acknowledgements

This thesis would have not been completed without the guidance, support, mentoring, and help from Dr. Alexandru Patriciu and Dr. Jim Reilly. I am thankful to Dr. Patriciu, especially for helping me choose courses, showing me ways to conduct research, instructing me in the biomedical design and surgical unit courses, allowing me to use and learn from data used in this thesis, guiding me with the data acquisition and statistical methods discussed in this thesis, and editing this thesis. I am also thankful to Dr. Reilly, especially for teaching me about matrix computations in signal processing, allowing me to use and learn from EEG data, guiding me with the machine learning method discussed in this thesis, and editing this thesis. I would like to thank Dr. Tim Davidson for teaching me the convex optimization method, which is also used in this thesis. Additionally, I would like to thank Dr. Bechir Hage and Dr. Anil Kapoor, who organized the volunteer surgeons, and all the volunteer surgeons for performing the tasks described in this thesis. I would also like to thank Dr. Shahram Shirani for giving me time to discuss the segmentation method used in this thesis.

Additional thanks go to Cheryl Gies and Dan Manolescu for all their friendly assistance during these three years. I am also grateful to my boss Gordon Hoops, Bruce Ohearon, and all employees from Candura Instruments for their constant support and understanding during my M.A.Sc studies. Special gratitude goes towards all my friends, especially, Ling Tsou, Hmwe Hmwe Kyu, Maryam Ravan, Pavneet Rehsi, Chen Xia, Qin Lei, Eleanor Leung, Li Hua Ying, Helen Huang, and Fanny Zhong for their help.

My deep gratitude goes to my Dad, U Sein Po, and Mum, Daw Ah Yin; sister, Khaing Yin Kyaw; and brother, Thet Naing Kyaw. I would like to rededicate this thesis to them and to all who shared their knowledge as well as skills.

Notation and abbreviations

PGY — Post graduate year

FLS — Fundamental of Laparoscopic Surgery curriculum

ANOVA1 — One-way analysis of variance

EMI — Electromagnetic interference sensors

${}^{H}\mathbf{p}_{tip}$ — Tip position vector referenced to handle frame

${}^{FT}\mathbf{o}_{H}$ — Instrument handle vector referenced to fixed transmitter frame

R — Rotation matrix

N — Total number of sample points

T — Total time taken to complete the entire task

t — Time index

|.| — Absolute value

subscript xl — Surgeon's left hand along the x-axis

subscript xr — Surgeon's right hand along the x-axis

subscript yl — Surgeon's left hand along the y-axis

subscript yr — Surgeon's right hand along the y-axis

subscript zl — Surgeon's left hand along the z-axis

subscript zr — Surgeon's right hand along the z-axis

||.|| — Two-norm formula

subscript nl — Surgeon's left hand using the norm formula

subscript nr — Surgeon's right hand using the norm formula

L with subscript — Trajectory length

Sp with subscript — Average speed

Sm with subscript — Smoothness

LF — Low frequency range from 0.1 Hz to 0.7 Hz

HF — High frequency range from 0.8 Hz to 30 Hz

R.H. — Right Hand

L.H. — Left Hand

subscript PFl — First peg picked from surgeon's left side

subscript PFr — First peg picked from surgeon's right side

subscript PLl — Last peg picked from surgeon's left side

subscript PLr — Last peg picked from surgeon's right side

subscript DFl — First peg dropped from surgeon's left side

subscript DFr — First peg dropped from surgeon's right side

subscript DLl — Last peg dropped from surgeon's left side

subscript DLr — Last peg dropped from surgeon's right side

N.L. — Neutral wrist stress level

M.L. — Moderate wrist stress level

S.L. — Severe wrist stress level

PCA — Principal component analysis

mRMR — Minimum redundancy and maximum relevance feature selection

FLD — Fisher linear discriminant

SVM — Support vector machine

m — no of sample dimensions

n — no of feature dimensions

r — no of reduced feature dimensions

$A \in \Re^{m \times n}$ — Training matrix data set with all measured samples and features

$A \in \Re^{m \times r}$ — Training matrix data set with all measured samples and reduced features

$\mathbf{x} \in \Re^{r}$ — Reduced feature vector

Contents

List of Figures

Chapter 1

Introduction and Problem Statement

In 1910, Hans Christian Jacobaeus performed the first laparoscopy on 17 patients (Hatzinger *et al.*, 2006). Since then, laparoscopy procedure has been optimized and simplified as a result of advance technology in optical delivery systems, minielectronic components and endoscopes (Atug *et al.*, 2006). The benefits of laparoscopy have also been well documented: reduced blood loss, less postoperative pain, shorter hospital stay, earlier return to normal activities, and improved cosmetics (McDougall and ClayMan, 1996).

While performing the laparoscopic surgery, surgeons insert a long instrument in the patient's belly through trocars that have a limited range of motion. Consequently, surgeons' hands tend to tremor while using laparoscopic tools. Because surgeons operate while looking at a monitor, there is a lack of depth perception. Consequently, the sense of touch development and hand-eye coordination require specific laparoscopic training (Derossis *et al.*, 1998). Ergonomic studies have shown a correlation between laparoscopic procedures and surgeon's pain in the region of neck and upper extremities (Berguer *et al.*, 1999). The shape of laparoscopic tool handles leads to muscle exhaustion, pressure areas, and neural injury as reported in the literature (Matern and Waller, 1999). Li (2002) has noted that awkward hand postures may lead to carpal tunnel syndrome, De Quervains disease and lateral epicondylitis. Many surgeons have complained of significant ergonomic

problems: frequent hand pains, wrist stiffness, finger numbness and eye-strain (Hemal *et al.*, 2001). Surgeons with less than two years of experiences in laparoscopic surgery are significantly more affected. Therefore, structure-based laparoscopic surgery training has become very important to provide patient safety (Lee *et al.*, 2011) and to avoid ergonomic risk factors for surgeons.

The Fundamental of Laparoscopic Surgery curriculum (FLS), endorsed by the American College of Surgeons, aims to teach the physiology, fundamental knowledge, and technical skills required in basic laparoscopic surgery (Derossis MD *et al.*, 1998). The FLS curriculum defines hand-eye coordination, ambidexterity, and depth perception as the basic skills required in laparoscopic surgery. Seven FLS training tasks, which include peg transfers, pattern cutting, clip and divide, endolooping, mesh placement and fixation, and suturing with intracorporeal or extracorporeal knots, are designed to teach these basic technical skills. All candidates are required to complete these training tasks successfully.

The non-surgery community is demanding that the curriculum be assessed. The assessment has to be a timely, unbiased, and an objective measurement of surgical skills (Darzi *et al.*, 1999). Ideally, the evaluation should be quantitative and automatic. The technical assessment methodology should be valid, reliable, and practical (Sidhu *et al.*, 2004). The assessment should provide numerical scores that reflect the technical skill level of a surgeon. It also should help a surgeon improve hand dexterity and hand movement precision. Furthermore, it could correct the surgeon's hand movements based on proper choreography taught by a surgical training institute. Moreover, it should provide feedback to the surgeon on the task execution ergonomics.

Reznick *et al.* (1997) has introduced a method of assessment using task-specific check-lists and global rating scales. Stations to perform the basic operations are used for the examination, and the skill performance at each station is marked by a qualified surgeon. The task-specific check-list comprises 20 to 40 required skill items, and the technical skills are assessed as either done correctly or done incorrectly. In the global rating scales, candidates are required to perform the basic operations at the stations and are graded on a five point scale by a qualified surgeon. Although the results of both methods have been proved to be reliable (Sidhu *et al.*, 2004), the methods have put the burden on expert surgeons, and the results have been highly subjective (Datta *et al.*, 2001; Moorthy *et al.*, 2003; Stylopoulos and Vosburgh, 2007).

Stylopoulos and Vosburgh (2007) has described a method of assessing technical skills using a motion analysis system. They have proved that the assessment of technical skills becomes more systematic, reproducible, and evaluator-independent by using the motion analysis method. Many motion analysis systems such as the Imperial College Surgical Assessment Device (ICSAD), ProMIS Augmented Reality Simulator (ProMIS), Robotic Video and Motion Analysis Software (ROVIMAS), and Hiroshima University Endoscopic Surgical Assessment Device (HUESAD) have also been reported to assess surgical technical skills (Mason *et al.*, 2012). The ICSAD system tracks surgeons' hand positions and movements using sensors placed on the dorsum of hands. The ProMIS system tracks instrument motion using three different camera tracking systems (Van Sickle *et al.*, 2005). The ROVIMAS system combines the ICSAD system with video-recording (Dosis *et al.*, 2005). The HUESAD system tracks the movements of the tip by utilizing optical scale sensors, micro-encoders and a computer (Egi *et al.*, 2008).

The Ascension 3DGuidance trakSTAR system also has the ability to track the position and orientation of an object in 3D space (trakStar, 2009). The system includes electromagnetic interference (EMI) sensors, a transmitter and an electronics interface unit to connect with a computer (trakStar, 2009). Riener *et al.* (2003) has utilized the system for recording an endoscope and arm movements during laparoscopy. Tausch *et al.* (2012) has used the system to track the motion of robotic instruments and validated robotic surgery curricula using the tracking system. Moreover, Zhou *et al.* (2013) has applied the 3DGuidance trakSTAR system for tracking catheter position during high-dose rate (HDR) prostate brachytherapy.

The use of a motion analysis system for assessing technical skills can be validated by a construct validity (Moorthy *et al.*, 2003). The construct validity is defined as a test that discriminates among various levels of expertise. Van Sickle *et al.* (2005) compared the hand dexterity of five novices and experts while the surgeons were performing a suturing task. The ProMIS system tracked the motion of two laparoscopic instruments and recorded time, smoothness, and path distance. Smoothness was defined as the number of changes in instrument velocity over time. These metrics were analysed using the Mann-Whitney U test. It was concluded that the experts performed the tasks between three and four times faster, had three times shorter instrument path length and had four times greater smoothness of instrument movement. Xeroulis *et al.* (2009) recruited 26 volunteer subjects

who were separated into three groups: 13 post graduate junior residents (PGY1,2,3), seven post graduate senior residents (PGY4,5) and six staff surgeons. All surgeons performed four FLS tasks: peg transfer task, pattern cut task, endoloop and intracorporeal suturing tasks. The total distance, number of movements and total time were recorded using ICSAD and analysed using one way of analysis (ANOVA1). There was a significant difference in the number of movements among experienced groups for peg transfer, endoloop and intracorporeal suturing tasks. The total distance was found to be a good discriminant for the experienced group for peg transfer and intracorporeal suturing tasks. The total time discriminated well between the two groups for all four tasks. It was also reported that there was a significant correlation between total FLS expert scores and the metrics of total distance, number of movements and total time. Datta *et al.* (2002) recruited fifty general surgical consultants and trainees to suture a synthetic vein patch to the artery with restricted access at depth. The number of hand movements and execution time were recorded using ICSAD and analysed using ANOVA1. There was a significant correlation between movements made and the global skills rating score.

Similar to the aforementioned results, several other researchers showed that motion analysis is a valid tool for assessing laparoscopic technical skills (Mason *et al.*, 2012). The time, path length and number of hand movements are valid metrics to assess technical skills. However, the overall effect of these parameters is not well addressed. Research on a method to convert the motion data into competency-based scores is on-going. Thus, the overall skill performance level based on the measured metric parameters is not predictable. Furthermore, the trajectory of the data from the motion analysis tool is not segmented. The current approach does not assess ergonomic analysis so that a surgeon can improve the ergonomics of handling instruments. We propose a system that acquires positions and orientation of movements, records these data, and converts these recorded data into a feedback training evaluation tool for laparoscopic surgeons. The system identifies the factors that differentiate the skill performance and wrist angles between novice and expert surgeons. Using these identified factors, it predicts whether a recorded trajectory is performed by a novice or an expert. The system also outputs a score that reflects the skill performance of a surgeon. Furthermore, it displays the segments of a recorded hand movement trajectory and includes ergonomic analysis on wrist angles.

Seven first year postgraduate (PGY1) urology residents, one general surgery resident (novice group), and eight fourth year postgraduate (PGY4) urology residents and fellows (expert group) volunteered to perform three trials of the peg transfer task and two trials of the suturing task with intracoporeal knots. They all read and signed the informed consent approved by the local ethics board. All volunteers were asked to use the same technique mentioned in the FLS guidelines. Because laparoscopic tools were inserted through small holes, which were about the same size as trocars, all volunteers performed the tasks with a limited range of motion. All volunteers also performed both tasks while looking at a monitor in direct line of a surgeon's vision. The Ascension 3DGuidance trakSTAR system was used to acquire the trajectories of the laparoscopic tools and angles of the surgeons' wrist. Custom software was developed to record the acquired data from the tracking system.

The recorded handle trajectory is transformed into the tip trajectory through calibration methods. The tip trajectory is then converted into factors that differentiate the skill performance between the novice and expert surgeons. Factors, such as total length, total time, average speed, and smoothness for the peg transfer task are analysed using ANOVA1 to assess how well they discriminate between the skill groups. The smoothness provides a measure of hand tremor and is defined as the ratio between low and high frequency trajectories. The factors, that are proved to distinguish the skill performance between two groups by ANOVA1 method, are used to calculate the skill performance-based score. The data are also analysed by using machine learning.

Machine Learning has been used in multiple disciplines: pattern recognition, data mining, statistics, probability theory, optimization, statistical physics, and theoretical computer science (Wang and Summers, 2012). Machine learning techniques such as rule induction, neural networks, genetic learning, case-based reasoning, and analytic learning have been used to solve real-world problems such as natural language processing, medical diagnosis, bioinformatics, video surveillance, or financial data analysis (Segre, 1992).

Machine learning techniques can be separated into three broad categories: supervised learning, unsupervised learning and semi-supervised learning (Wang and Summers, 2012). In supervised learning, each sample contains two vectors: a set of features and a label vector. For example, a sample is the trajectory of a surgeon's hand movement; features, relevant for surgeon's skill, are

extracted from a sample (Alpaydin, 2010). Labels contain objective values relevant to the problem at hand. For example, a PGY1 laparoscopic resident is labelled as -1 whereas a urology fellow is labelled as +1. Supervised learning attempts to determine the relationship between a set of features and a label (Wang and Summers, 2012). Examples of supervised learning are classification, regression, and reinforcement learning.

In unsupervised learning, each sample contains only a set of features. Unsupervised learning determines the relationships between samples. Examples of unsupervised learning are clustering, density estimation, and blind source separation. Semi-supervised learning is the combination of both supervised learning and unsupervised learning. In semi-supervised learning, some samples contain labels, and many of the samples do not contain labels. Semi-supervised classification and information recommendation systems are examples of semi-supervised learning. Based on the applications, machine learning has different modules (Segre, 1992). For example, a pattern classification generally includes three modules: feature extraction, feature selection and classification.

Our application employs supervised learning and comprises five modules: hand trajectory segmentation, feature extraction, feature selection, classification, and evaluation. Hand trajectory segmentation has been used in research areas such as neuroscience, robotics, and ergonomics (Faria and Dias, 2009). The skill to manipulate objects with our hands is the result of a sophisticated blend of automatic sensory-motor mechanisms (Johansson and Cole, 1992). A hand manipulation task is segmented into different stages: reach, lift, transport and release (Flanagan *et al.*, 2006). Then, features such as the number of up and down movements, length, time, average speed, and smoothness are extracted. Subsequently, the features that are most statistically related with labels are selected using either principal component analysis (PCA) or minimum redundancy and maximum relevance feature selection (mRMR) (Wang and Summers, 2012). The best features are used to calculate the skill performance-based score.

The classifier is built to distinguish the skill performance between novice and expert surgeons. Two types of classifiers are used: Fisher linear discriminant (FLD) and support vector machine (SVM). Each classifier can be combined with any feature selection method resulting in four investigated models for surgeon skill performance prediction. The performance of each model was evaluated using a leave-n-out cross validation procedure (Khodayari-Rostamabad *et al.*, 2013).

Both ANOVA1 and machine learning methods are applied in ergonomic analysis of surgeons' wrist angles while the surgeons are performing both the peg transfer and suturing task. EMI sensors are attached on wrists and forearms to monitor the surgeons' wrist angles. The wrist angles are grouped according to surgeon's wrist postures: extension, flexion, radial deviation and ulnar deviation. The wrist postures are further grouped based on stress level: neutral, moderate and severe. The percentage duration on each stress level for each wrist posture is calculated to give feedback to surgeons. The percentage duration is also used to define factors for ANOVA1 and features for machine learning. Factors that identify wrist angle differences between the novice and expert surgeons are used to validate the motion analysis system for tracking surgeons' wrist movements. Features are applied in the same four models that are proposed in the skill performance prediction to analyse surgeons' ergonomic performance on wrist angles. Each model is also evaluated using the leave-n-out cross validation procedure.

1.1 Thesis Contribution

Dr. Patriciu proposed and implemented the system of measuring the laparoscopic tip motion, hand, forearms, elbows movements and wrist angles using Ascension 3DGuidance trakSTAR. Dr. Bechir Hage and Dr. Anil Kapoor organized the seven PGY1 laparoscopic residents and one general surgery resident and the eight PGY4 urology residents and fellows that perform three tirals of the peg transfer task and two trials of the suturing task. Dr. Reilly contributed the smoothness factor, which is intended to measure hand tremor. Under the guidance of Dr. Patriciu, the author proved that the factors discriminate the skill performance between novice and expert surgeons. Thus, the Ascension 3DGuidance trakSTAR system for tracking laparoscopic tip motion was validated. Under the supervision of Dr. Patriciu and Dr. Reilly, the author implemented the hand trajectory segmentation. Under the guidance of Dr. Reilly, the author implemented feature extraction, feature selection, classification, and evaluation. The machine learning approach discriminated between experts and novices correctly in 73% of cases. The author derived a competency-based surgeon score using the results from either the statistical or the machine learning method. Using the statistical method, the author analysed the stress level of surgeons' wrist angles and validated the system of measuring surgeons' wrist angles using Ascension 3DGuidance trakSTAR. Using the machine learning approach,

the stress level of surgeons' wrist angles between experts and novices was discriminated correctly in 88% of the cases for the peg transfer task and in 75% of the cases for the suturing task.

1.2 Organization of Thesis

Chapter 2 describes the standard tasks used in this study: the methods applied to acquire laparoscopic instrument trajectories and surgeons' wrist angles during the task execution. Chapter 3 discusses the statistical method used for validating motion analysis and skill evaluation. Chapter 4 presents the machine learning method to predict the skill performance of a surgeon. Chapter 5 provides some results related to ergonomic analysis of wrist angles. Chapter 6 discusses the conclusions regarding the results and provides some future research directions.

Chapter 2

Data Acquisition

As depicted in Figure 2.1, Chapter 2 describes the standard tasks used in this study: the methods applied to acquire laparoscopic instrument trajectories and surgeons' wrist angles during the task execution. Seven PGY1 laparoscopic residents and one general surgery resident (novice group) and eight PGY4 residents and urology fellows (expert group) performed three trials of the peg transfer task and two trials of the suturing task using the laparoscopic tools. The Ascension 3DGuidance trakSTAR system tracks the position and orientation of laparoscopic handles in surgeons' hands and the orientation of surgeons' wrists angles. The acquired data are recorded by custom software. The recorded laparoscopic handle data are then converted into a tip trajectory through estimating the tip positions referenced to the handle positions by either eigenvalue decomposition or a pivot-calibration method. Similarly, the recorded surgeons' wrist angles are converted into ergonomic assessment data.

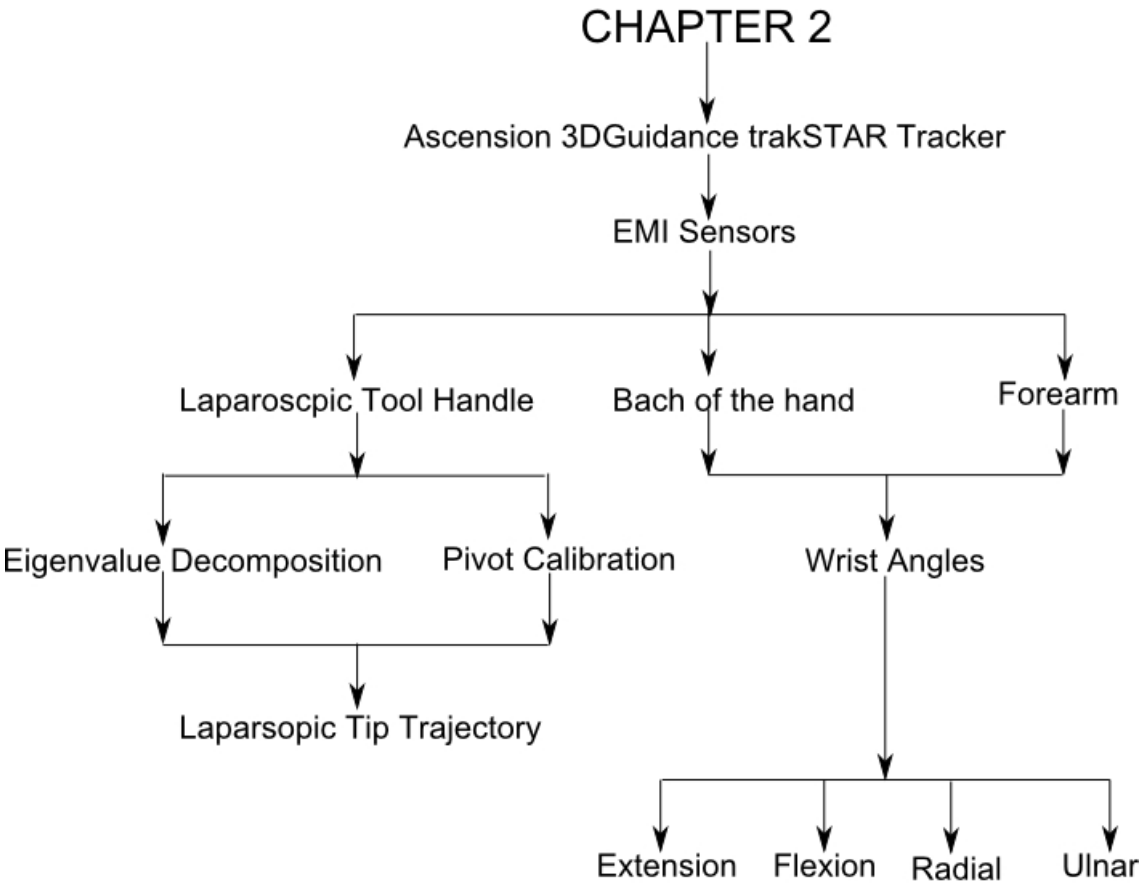

Figure 2.1: Chapter 2 Outline

2.1 System Set-up and Performance Guideline for Peg Transfer Task

The system set-up for the peg transfer task comprised two laparoscopic graspers (Figure 2.2) fitted with trakStar micro-EMI sensors, the trakStar tracking system, three blue and two pink triangles on a dexterity block, and a standard FLS trainer system station (Figure 2.3) (Figure 2.4) which contained the top of the trainer with simulated skin with two holes, base of the trainer with alligator clips, two side panels, and a FLS standard four millimetres fixed focus lens swivel mounted camera. The dexterity block was placed in the centre field of the camera's view. Five pegs were placed on the pegboard on the surgeon's left side and arranged in the order of the closest to the most distant from the transmitter.

By viewing the monitor, the surgeons manipulated the two laparoscopic graspers inserted into small holes, which were about the same size as trocars. Each peg was lifted with the grasper in the surgeon's left hand, transferred to the surgeon's right hand in mid-air, and lastly it was placed on the right side in the same arrangement as the right side (Derossis *et al.*, 1998). After all five pegs from the surgeon's left side were transferred to the right side, they were moved back to surgeon's left side in a first-in, first-out order.

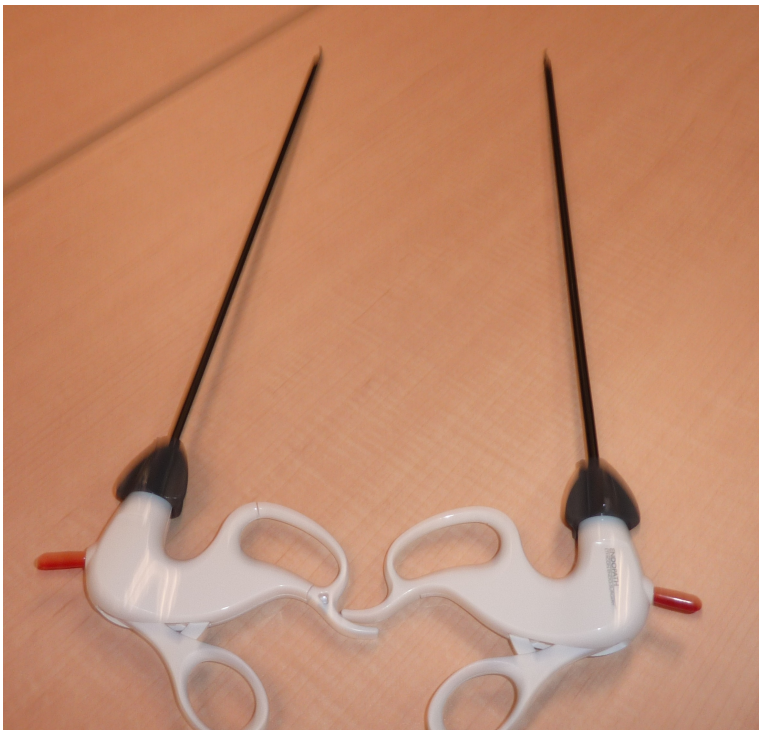

Figure 2.2: Graspers that were used in the Peg Transfer Task

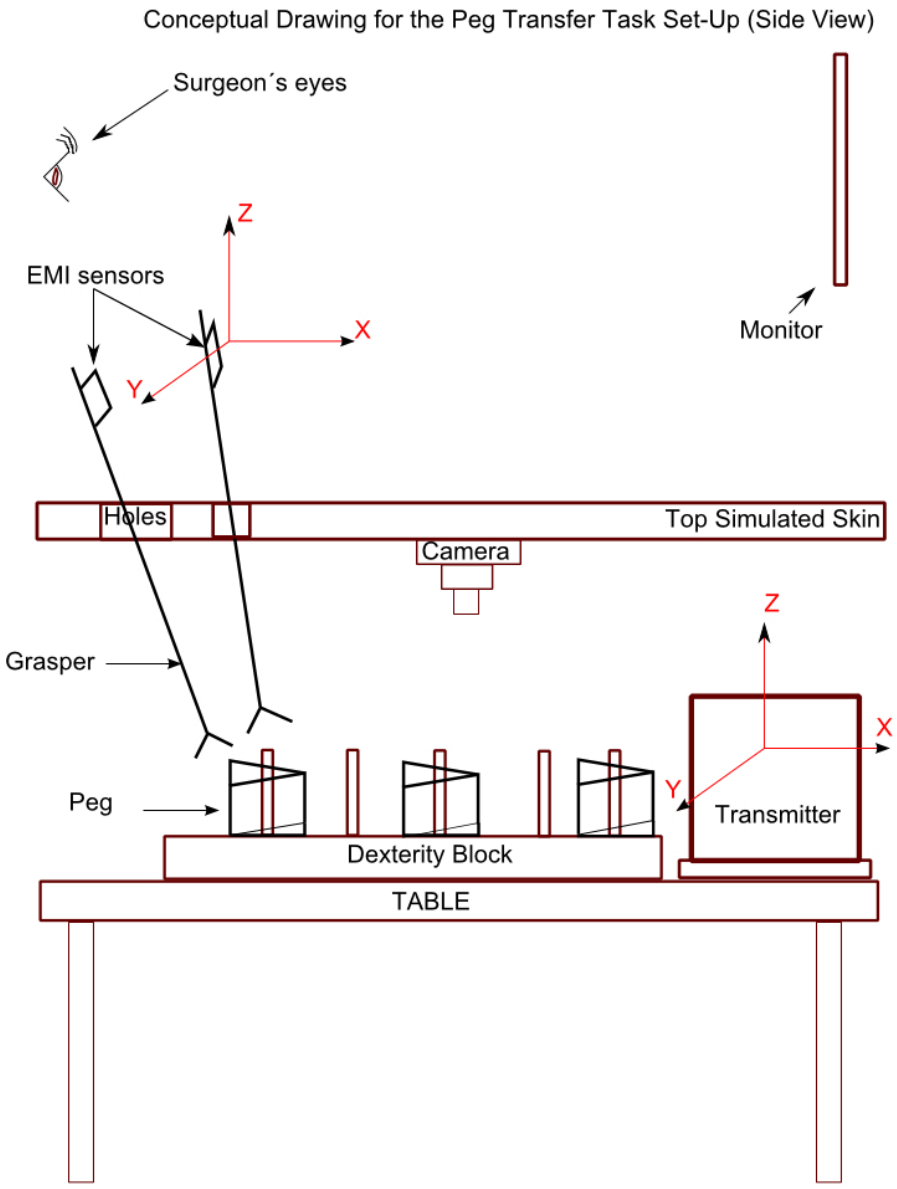

Figure 2.3: Conceptual Drawing for the Peg Transfer Task Set-Up

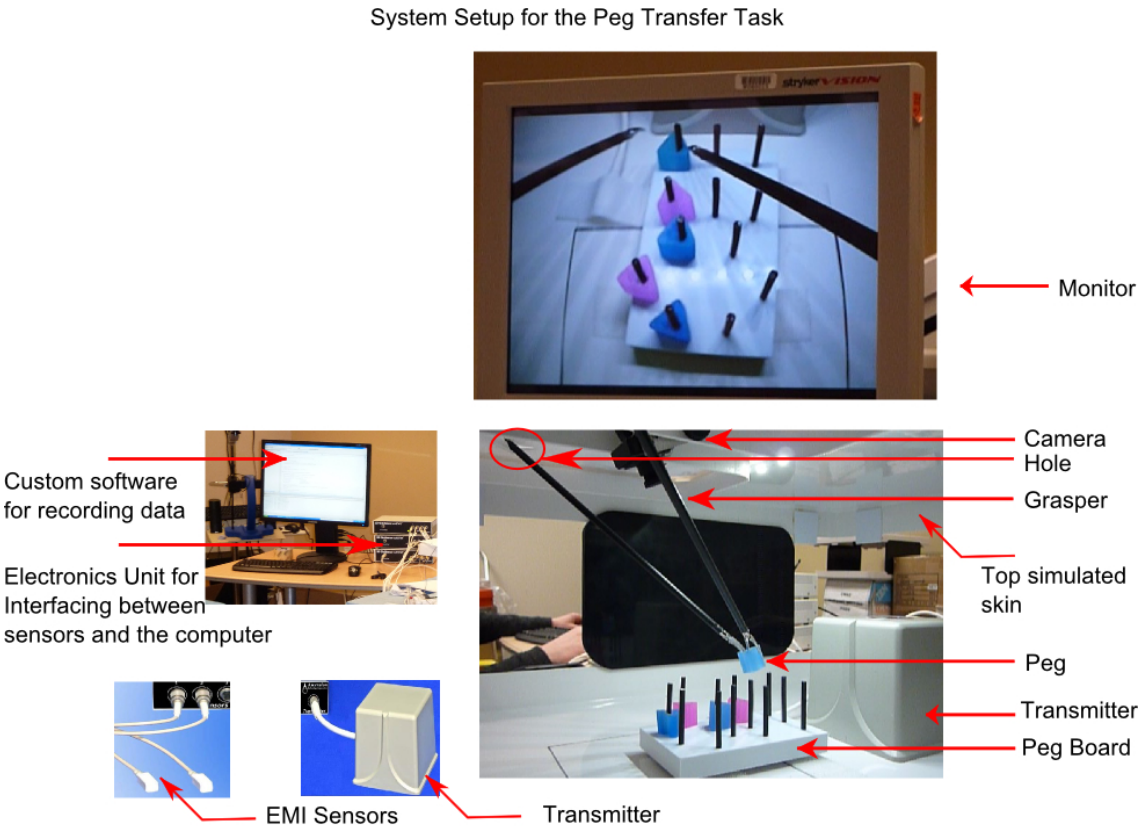

Figure 2.4: System Set-Up for the Peg Transfer Task

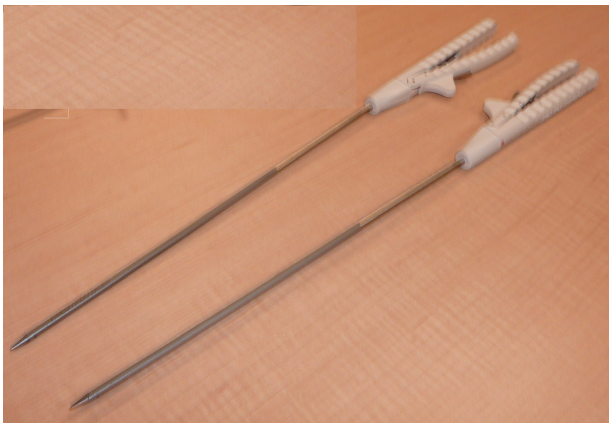

Figure 2.5: Needle-Drivers that were used in the Suturing Task

2.2 System Set-up and Performance Guideline for Suturing Task

The system set-up for the suturing task comprised two needled drivers (Figure 2.5) fitted with optical sensors, the same FLS trainer system station that is used in the peg transfer task, a Penrose Drain with marked targets placed firmly on a suture block, and the custom tracking system. The suture block was placed in the centre field of the camera's view. By viewing the monitor, a simple stitch was placed through two marks in a longitudinally slit Penrose drain. The suture was tied using an intracorporeal knot technique. Three throws that included one double throw and two single throws were placed on the suture.

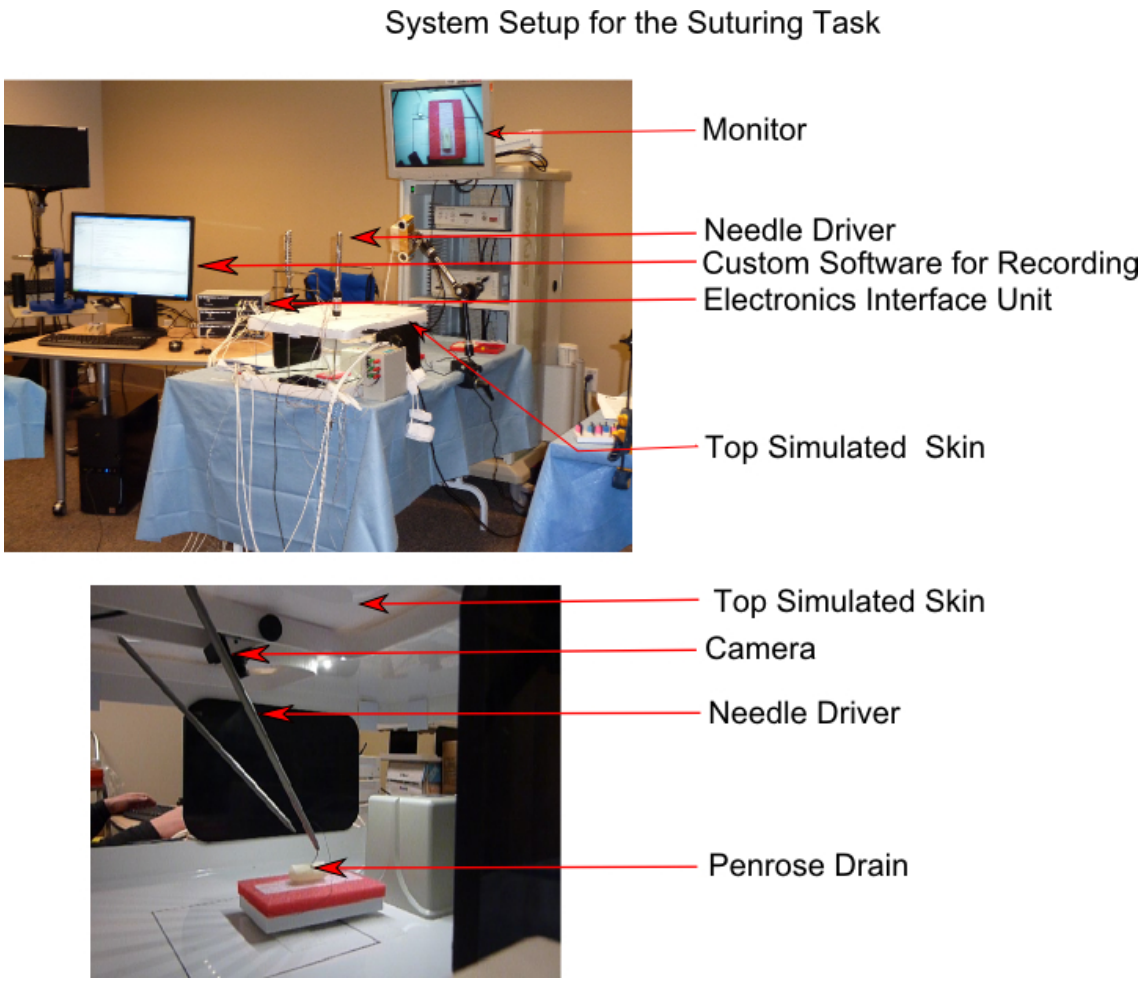

Figure 2.6: System Setup for the Suturing Task

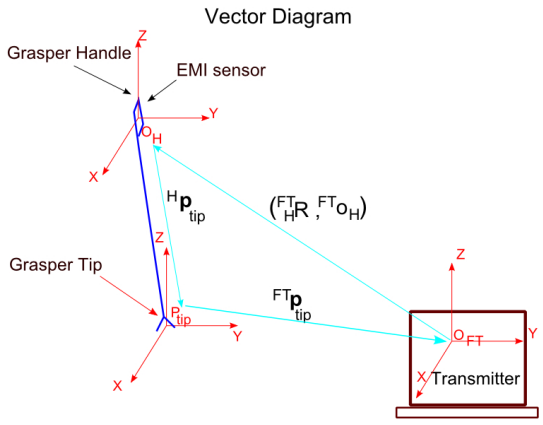

Figure 2.7: Vector Diagram for Formula 2.1

2.3 Data Acquisition for Skills Evaluation on the Peg Transfer Task

Both grasper handles in surgeons' right and left hands are fitted with the EMI sensors. The transmitter sequentially generates magnetic fields and the EMI sensors instantly measure the transmitted field vectors at a point in space (trakStar, 2009). Thus, the positions and orientations of the handle (subscript or superscript H) referenced to the fixed transmitter (superscript FT) are captured and recorded using custom software. Formula 2.1 provides the tip positions (subscript tip) of the grasper with respect to the fixed transmitter ($^{FT}\mathbf{p}_{tip}$) (Mercier *et al.*, 2005). Figure 2.7 shows the vector diagram for Formula 2.1.

$$^{FT}\mathbf{p}_{tip} = \; {}^{FT}_{H}R \; {}^{H}\mathbf{p}_{tip} \; + \; {}^{FT}\mathbf{o}_{H} \; , where \tag{2.1}$$

$${}^{FT}_{H}R = \; {}^{FT}_{H}R_z(\psi) \; . \; {}^{FT}_{H}R_y(\theta) \; . \; {}^{FT}_{H}R_x(\phi) \tag{2.2}$$

$${}^{FT}_{H}R = \begin{pmatrix} \cos(\theta_H)\cos(\psi_H) & \cos(\phi_H)\sin(\psi_H) + \sin(\phi_H)\sin(\theta_H)\cos(\psi_H) & \sin(\phi_H)\sin(\psi_H) - \cos(\phi_H)\sin(\theta_H)\cos(\psi_H) \\ -\cos(\theta_H)\sin(\psi_H) & \cos(\phi_H)\cos(\psi_H) - \sin(\phi_H)\sin(\theta_H)\sin(\psi_H) & \sin(\phi_H)\cos(\psi_H) + \cos(\phi_H)sin(\theta_H)sin(\psi_H) \\ \sin(\theta_H) & -\sin(\phi_H)\cos(\theta_H) & \cos(\phi_H)\cos(\theta_H) \end{pmatrix}$$

$^{FT}\mathbf{p}_{tip}$ are the tips positions of the instruments with respect to the fixed transmitter coordinate

system.

${}^{FT}\mathbf{o}_H$ are the positions of the handles with respect to the fixed transmitter coordinate system.

${}^{H}\mathbf{p}_{tip}$ are the positions of the tips with respect to the instrument coordinate sensor. This is computed using either the Eigenvalue Decomposition Method or the pivot calibration method (PCM) which are explained details in the following subsections.

2.3.1 Instrument Tip Position Calibration Using the Eigenvalue Decomposition Method

The tip position referenced to the instrument's sensor is estimated using the following method.

1. Rotate the instrument while keeping the tip at one specific location ${}^{FT}\mathbf{p}_{tip}$. The instrument sensor will describe partial arcs of the sphere patterns. Consequently, the recorded data are perpendicular to the main axis of the grasper (Figure 2.8).

2. The custom software stores the positions of the grasper handle in the form of x_{Hi}, y_{Hi}, z_{Hi}, ϕ_{Hi}, θ_{Hi} and ψ_{Hi}, where i=1,...,N.

3. Then, ${}^{H}\mathbf{p}_{tip}$ is computed by solving the following overdetermined equation:

$$\begin{pmatrix} {}^{FT}_{H}R_1 \\ {}^{FT}_{H}R_2 \\ . \\ . \\ . \\ {}^{FT}_{H}R_N \end{pmatrix} {}^{H}\mathbf{p}_{tip} = \begin{pmatrix} {}^{FT}\mathbf{p}_{tip} - {}^{FT}\mathbf{o}_{H1} \\ {}^{FT}\mathbf{p}_{tip} - {}^{FT}\mathbf{o}_{H2} \\ . \\ . \\ . \\ {}^{FT}\mathbf{p}_{tip} - {}^{FT}\mathbf{o}_{HN} \end{pmatrix}$$

where, Formula 2.2 provides ${}^{FT}_{H}R_i$, ${}^{FT}\mathbf{o}_{Hi} = (x_{Hi}, y_{Hi}, z_{Hi})^T$. The next section provides the algorithm used to compute ${}^{FT}\mathbf{p}_{tip}$.

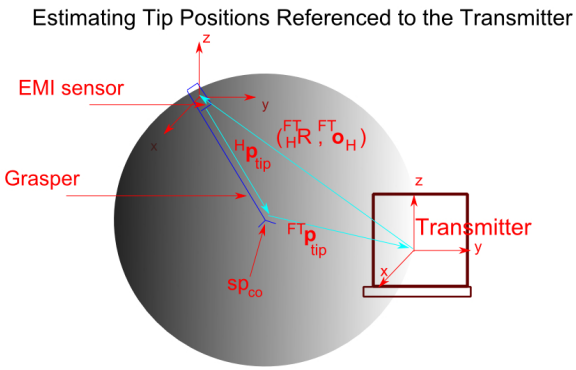

Figure 2.8: Estimating Tip Positions Referenced to the Transmitter

Pivoting Point ($^{FT}\mathbf{p}_{tip}$) Estimation

1. Compute the centroid of the point cloud; subtract the centroid from each point

$$\bar{x} = \frac{1}{N}\sum_{i=1}^{N}\mathbf{x}_i \quad \bar{y} = \frac{1}{N}\sum_{i=1}^{N}\mathbf{y}_i \quad \bar{z} = \frac{1}{N}\sum_{i=1}^{N}\mathbf{z}_i$$

$$\tilde{x_i} = x_i - \bar{x} \quad \tilde{y_i} = y_i - \bar{y} \quad \tilde{z_i} = z_i - \bar{z}$$

2. Compute the covariance matrix, which is formed by

$$C = \sum_{i=1}^{N}\begin{bmatrix} \tilde{x_i}^2 & \tilde{x_i}\tilde{y_i} & \tilde{x_i}\tilde{z_i} \\ \tilde{x_i}\tilde{y_i} & \tilde{y_i}^2 & \tilde{y_i}\tilde{z_i} \\ \tilde{x_i}\tilde{z_i} & \tilde{y_i}\tilde{z_i} & \tilde{z_i}^2 \end{bmatrix}$$

3. Compute the eigenvector and eigenvalues of the covariance matrix C.

4. The eigenvectors of all the large eigenvalues of the covariance matrix point to the principal directions of the data whereas the eigenvector $\mathbf{v} = [v_x \ v_y \ v_z]$ of the smallest eigenvalues of the covariance matrix points to the main axis of the grasper. Thus, the initial estimation of the tip positions $< x_{co}, y_{co}, z_{co} >$ referenced to the transmitter is obtained by calculating the centre and radius of a sphere (R_{spo}):

$$x_{co} = \bar{x} + v_x.L$$

$$y_{co} = \bar{y} + v_y.L$$

$$z_{co} = \bar{z} + v_z.L$$

$$R_{spo} = L$$

where L is an approximation of the distance between the instrument attached sensor coordinate system and the instrument's tip.

5. These values are used as a starting point in a non-linear least square fit function.

$$\underset{\mathbf{x}}{\text{minimize}} \quad ||f(\mathbf{x})||_2^2$$

,where $\mathbf{x}$=$[x_c, y_c, z_c, R_{sp}]$

$f(x_c, y_c, z_c, R_{sp}) = [R_{sp1} - R_{sp},\ R_{sp2} - R_{sp},\ ...,\ R_{spN} - R_{sp}]^T = \left\| \begin{matrix} x_c - x_i \\ y_c - y_i \\ z_c - z_i \end{matrix} \right\|_2^2$ where i=1,2,3,...,N

The non-linear least squares problem was solved using lsqnonlin built in MATLAB's Simulink®.

6. ${}^{FT}\mathbf{p}_{tip} = [x_c, y_c, z_c]^T$

2.3.2 Tip Position (${}^{H}\mathbf{p}_{tip}$) Estimation through Pivot Calibration Method

Alternatively, the tip position referenced to the grasper's handle is estimated using the classical PCM comprising the following method.

1. Rotate the instrument while keeping the tip at one location ${}^{FT}\mathbf{p}_{tip}$.

2. The custom software stores the positions of the grasper handle in the form of x_{Hi}, y_{Hi}, z_{Hi}, ϕ_{Hi}, θ_{Hi} and ψ_{Hi}, where i=1,...,N.

3. The position of the instrument's tip with respect to the fixed transmitter is

$${}^{FT}\mathbf{p}_{tip} = ({}^{FT}_{H}R_i)\ {}^{H}\mathbf{p}_{tip}\ +\ {}^{FT}\mathbf{o}_{Hi}\ where\ i = 1, ..., N \tag{2.3}$$

4. Add Equation 2.3 for $i = 1, ..., N$ and divide by N.

$$ {}^{FT}\mathbf{p}_{tip} = (\frac{1}{N}\sum_{i=1}^{N} {}^{FT}_{H}R_i)\ {}^{H}\mathbf{p}_{tip} + (\frac{1}{N}\sum_{i=1}^{N} {}^{FT}\mathbf{o}_{Hi}) \tag{2.4} $$

5. Subtract Equation 2.4 from Equation 2.3 for $i = 1, ..., N$; this will eliminate the unknown ${}^{FT}\mathbf{p}_{tip}$

$$ 0 = ({}^{FT}_{H}R_i \ - \ \frac{1}{N}\sum_{i=1}^{N} {}^{FT}_{H}R_i)\ {}^{H}\mathbf{p}_{tip} + ({}^{FT}\mathbf{o}_{Hi}) \ - \ (\frac{1}{N}\sum_{i=1}^{N} {}^{FT}\mathbf{o}_{Hi}) \, , where\ i = 1, ..., N \tag{2.5} $$

Equation 2.5 is rearranged as

$$ \begin{pmatrix} {}^{FT}_{H}R_1 \ - \ \frac{1}{N}\sum_{i=1}^{N} {}^{FT}_{H}R_i \\ {}^{FT}_{H}R_2 \ - \ \frac{1}{N}\sum_{i=1}^{N} {}^{FT}_{H}R_i \\ \cdot \\ \cdot \\ \cdot \\ {}^{FT}_{H}R_N \ - \ \frac{1}{N}\sum_{i=1}^{N} {}^{FT}_{H}R_i \end{pmatrix} {}^{H}\mathbf{p}_{tip} = \begin{pmatrix} \sum_{i=1}^{N} {}^{FT}\mathbf{o}_{Hi} \ - \ {}^{FT}\mathbf{o}_{H1} \\ \sum_{i=1}^{N} {}^{FT}\mathbf{o}_{Hi} \ - \ {}^{FT}\mathbf{o}_{H2} \\ \cdot \\ \cdot \\ \cdot \\ \sum_{i=1}^{N} {}^{FT}\mathbf{o}_{Hi} \ - \ {}^{FT}\mathbf{o}_{HN} \end{pmatrix} \tag{2.6} $$

6. ${}^{H}\mathbf{p}_{tip}$ is obtained by solving over constrained Equation 2.6.

2.4 Data Acquisition for Ergonomic Analysis on the Peg Transfer Task and the Suturing Task

While manipulating the grasper handles for both tasks, the surgeons' wrist postures are exposed to extension, flexion, ulnar deviation and radial deviation. Wrist flexion (Θ_{FLEX}) is defined as moving the palm of the hand toward the front of the forearm, whereas wrist extension (Θ_{EXT}) is defined as moving the back of the hand toward the back of the forearm. Wrist ulnar deviation (Ψ_{ULN}) is defined when the hand including the fingers moves towards the ulna; whereas wrist radial deviation (Ψ_{RAD}) is defined when the hand including the fingers moves towards the radius. The surgeons wrist angles are measured by using two EMI sensors: one mounted on the forearm and the second one mounted on the back of the hand as shown in Figure 2.9. The axes of the two sensors are parallel to each other when the hand is at the steady posture. The extension and flexion are measured as the angle differences between sensors on the forearm and the back of the hand along the y-axis (Figure 2.10). Wrist extension results in positive angles along the y-axis, whereas wrist flexion results in negative angles along the y-axis. The ulnar and radial deviations are measured as the angle differences between sensors on the forearm and the back of the hand along the z-axis (Figure 2.11). Wrist ulnar deviation results in positive angles along the z-axis whereas wrist radial deviation results in negative angles along the z-axis.

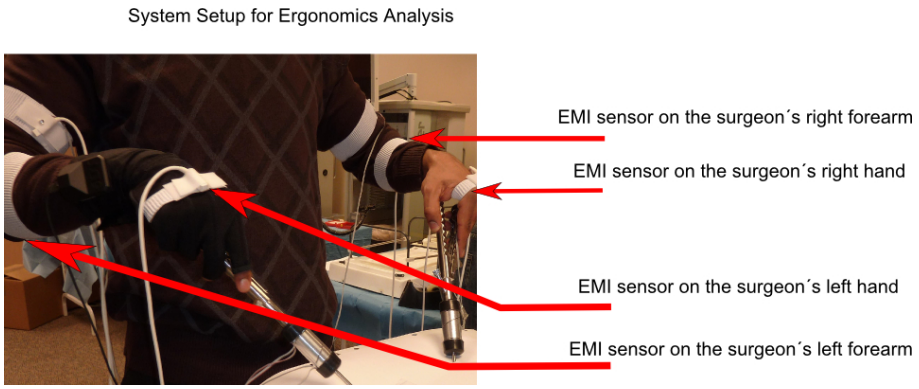

Figure 2.9: System Setup for Ergonomic Analysis

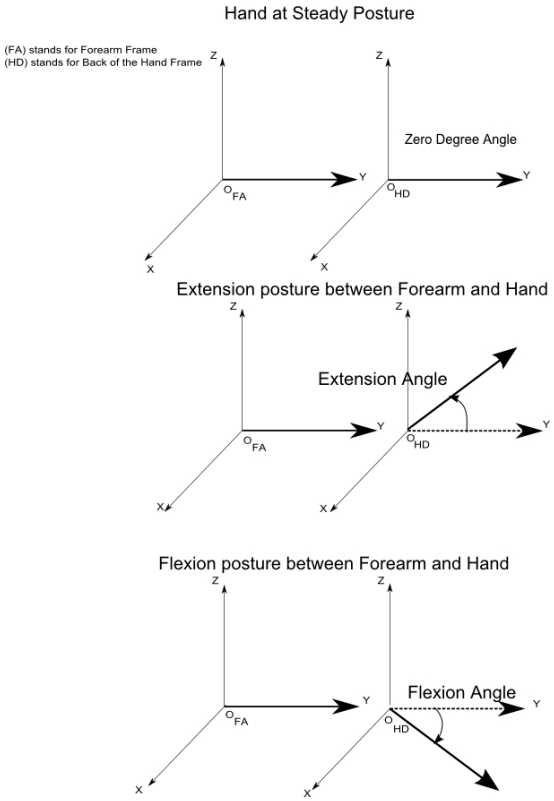

Figure 2.10: Extension/Flexion Measurement

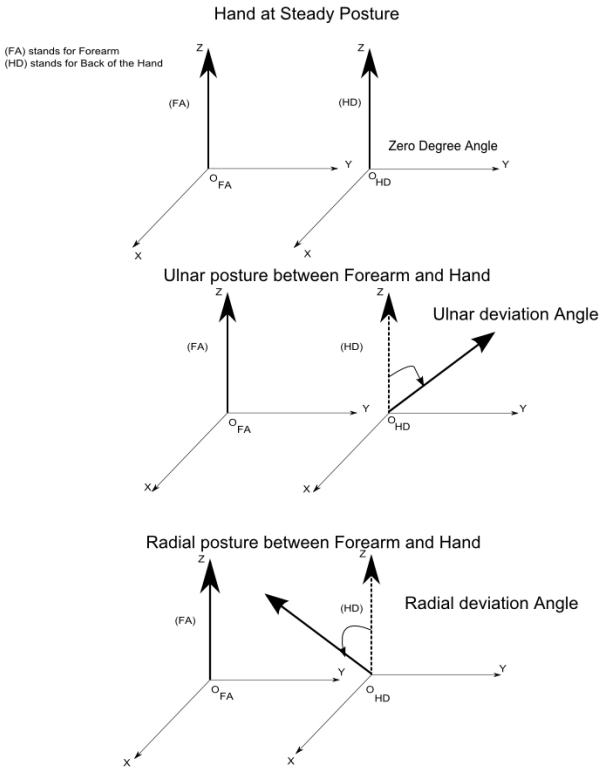

Figure 2.11: Ulnar/Radial Measurement

Chapter 3

Statistical Approach and Results

A statistical approach is used to validate the Ascension 3DGuidance trakSTAR system for tracking the tip movements of laparoscopic tools and to quantify the differences on the skill performance between novice and expert surgeons for the peg transfer task. Figure 3.1 outlines the steps for analysing the data using the statistical approach (Ropella, 2007). Firstly, factors that may contribute to the skill performance between novice and expert surgeons are proposed. Secondly, using these factors, hypotheses are formulated to determine whether the skill performance between novice and expert surgeons is distinguishable. Thirdly, a probability model is assumed to make a decision on accepting or rejecting hypotheses. Lastly, the hypothesis with one factor at a time is tested using ANOVA1. The goal of ANOVA1 is to test for differences among the means of surgeons' skill levels and to quantify these differences. The factors rejected by the hypotheses are proved to statistically distinguish the skill performance between novice and expert surgeons. Because the factors discriminate the skill performance between novice and expert surgeons, the Ascension 3DGuidance trakSTAR system for tracking the tip movements of laparoscopic tools is validated. The competency-based scores for all surgeons are achieved using these factors.

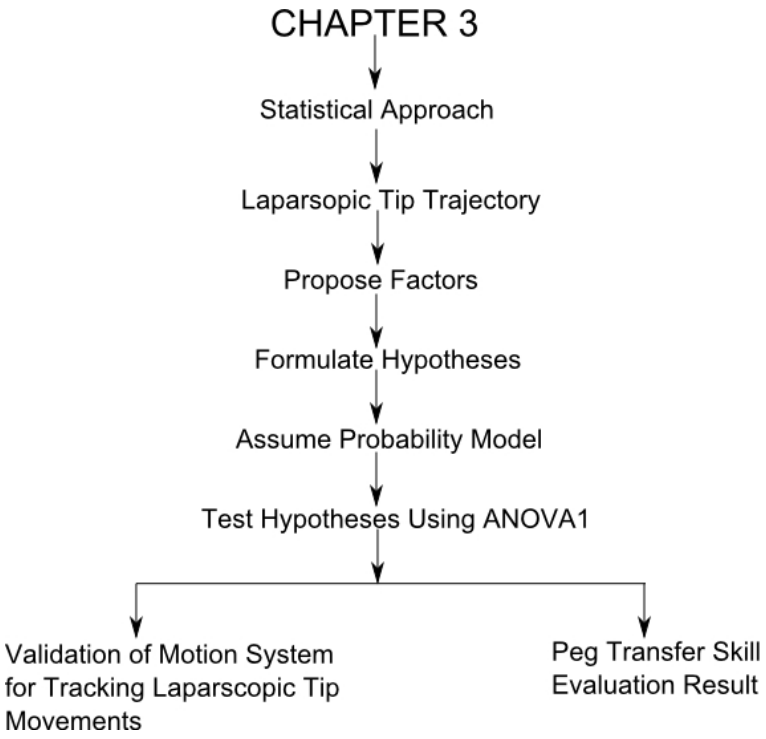

Figure 3.1: Chapter 3 Outline

3.1 Factors

Factors that may contribute to the skill performance between novice and expert surgeons are separated into four categories: path length, time, average speed and smoothness. The following explains each category.

- **Path Length:** Path length is defined as the total distance travelled by the tip of the laparoscopic tool in a surgeon's hand while performing the entire task. Falcone *et al.* (2012) reported that there are over 268 trillion ways of completing the peg transfer task. Path length is found to be inversely related to the degree of economy of motion. The economy of motion is defined as the minimum hand movements required to complete a task (Barnes and Barnes, 1958).

- **Time:** Time is defined as the time required to complete the entire task. The time factor is inversely related to the surgical efficiency. The surgical efficiency is defined as the cost to complete the entire task.

- **Average Speed:** Average speed is the ratio of path length to time. It is directly related to the surgical efficiency.

- **Smoothness:** Smoothness is defined as the ratio of low to high frequency components of the tip trajectory. The frequency measurements of laparoscopic tip movements are obtained by using a Fast Fourier transform algorithm. The threshold value between low and high frequencies is obtained through the experiment on the degree of differentiating the skill performance between novice and expert surgeons. Thus, this value may just apply to these acquired data. The low frequency range is from 0.1Hz to 0.7Hz whereas the high frequency range is from 0.8Hz to 30Hz. The smoothness factor is intended to be used as the measurement of hand tremor. A higher smoothness value is assumed to have less hand tremor or volitional jerky movements. The norm formula used in the smoothness factor $\mathrm{HF_{nr}}, \mathrm{HF_{nl}}, \mathrm{LF_{nr}}, \mathrm{LF_{nl}}$ is obtained by first converting three dimensional space to one dimensional space using the norm formula $\sqrt{x_i^2 + y_i^2 + z_i^2}$ where $i = 1, 2, ..., N$.

Path length, time and average speed can also be used to differentiate the skill performance between novice and expert surgeons and to validate the motion system (Mason *et al.*, 2012). Each

category is further grouped into the measurements along the x-axis, y-axis, z-axis and the measurement using the norm formula. The measurement along the x-axis contributes to the analysis of the path of detecting the positions of pegs. The measurement along the y-axis contributes to the analysis of the path of transferring pegs. The measurement along the z-axis contributes to the analysis of the path of picking or dropping pegs. The measurement using the norm formula contributes to analysis of the overall effect of the measurements along the x-axis, y-axis and z-axis. All these factors are listed in Table 3.1:

Table 3.1: Factor Definition

Description	Symbol	Side	Definition	Justification	Unit
Path Length	L_{xr}	R.H.	$\sum_{i=1}^{N-1} \lvert x_i - x_{i+1} \rvert$	Economy	centimetre
	L_{yr}	R.H.	$\sum_{i=1}^{N-1} \lvert y_i - y_{i+1} \rvert$		
	L_{zr}	R.H.	$\sum_{i=1}^{N-1} \lvert z_i - z_{i+1} \rvert$		
	L_{nr}	R.H.	$\sqrt{L_{xr}^2 + L_{yr}^2 + L_{zr}^2}$		
	L_{xl}	L.H.	$\sum_{i=1}^{N-1} \lvert x_i - x_{i+1} \rvert$		
	L_{yl}	L.H.	$\sum_{i=1}^{N-1} \lvert y_i - y_{i+1} \rvert$		
	L_{zl}	L.H.	$\sum_{i=1}^{N-1} \lvert z_i - z_{i+1} \rvert$		
	L_{nl}	L.H.	$\sqrt{L_{xl}^2 + L_{yl}^2 + L_{zl}^2}$		
Total Time	T	-	$t_N - t_1$	Efficiency	second
Average Speed	Sp_{xr}	R.H.	$\frac{1}{T} L_{xr}$	Efficiency	$\frac{\text{centimetre}}{\text{second}}$
	Sp_{yr}	R.H.	$\frac{1}{T} L_{yr}$		
	Sp_{zr}	R.H.	$\frac{1}{T} L_{zr}$		
	Sp_{nr}	R.H.	$\frac{1}{T} L_{nr}$		
	Sp_{xl}	L.H.	$\frac{1}{T} L_{xl}$		
	Sp_{yl}	L.H.	$\frac{1}{T} L_{yl}$		
	Sp_{zl}	L.H.	$\frac{1}{T} L_{zl}$		
	Sp_{nl}	L.H.	$\frac{1}{T} L_{nl}$		
Smoothness	Sm_{xr}	R.H.	$\frac{LF_{xr}}{HF_{xr}}$	Hand tremor	unitless
	Sm_{yr}	R.H.	$\frac{LF_{yr}}{HF_{yr}}$		
	Sm_{zr}	R.H.	$\frac{LF_{zr}}{HF_{zr}}$		
	Sm_{nr}	R.H.	$\frac{LF_{nr}}{HF_{nr}}$		
	Sm_{xl}	L.H.	$\frac{LF_{xl}}{HF_{xl}}$		
	Sm_{yl}	L.H.	$\frac{LF_{yl}}{HF_{yl}}$		
	Sm_{zl}	L.H.	$\frac{LF_{zl}}{HF_{zl}}$		
	Sm_{nl}	L.H.	$\frac{LF_{nl}}{HF_{nl}}$		

3.2 Hypotheses Formulation

Applying the factors listed in Table 3.1, the following null hypotheses are formulated:

1. The means of the path length factors in the expert and novice groups are the same.
2. The means of the total time factor in the expert and novice groups are the same.
3. The means of the average speed factors in the expert and novice groups are the same.
4. The means of the smoothness factors in the expert and novice groups are the same.

3.3 Probability Model

A probability model describes the likelihood of the occurrence of an experimental outcome and the characteristics of the population. For example, a probability model of the time factor for the novice surgeons predicts the most likely time that any novice takes to complete the entire task. Because there are eight subjects for each group, insufficient data are acquired to predict the probability model. Therefore, according to the central limit theorem, which states that the sum of random processes with arbitrary distributions will result in a random variable with a normal distribution, each factor is modelled as the normal distribution. The variance in the two populations for each factor is assumed to be the same. The two populations are assumed to be mutually independent.

3.4 Hypotheses Testing

With the assumptions made in the probability model section, the one-way analysis (ANOVA1) can be used to test the hypothesis by applying one factor at a time: $H_0 : \mu_J = \mu_E$ (Devore, 2012). The subscript J refers to the novice group whereas the subscript E refers to the expert group. Each observation is written as $x_{ij} = \mu_i + \epsilon_{ij}$, $i \in \{J, E\}$ where ϵ_{ij} measures the deviation of the j^{th} observation from the corresponding mean group. The p-value is used to quantify the differences in the means of two groups: it is inversely related to the confidence level of rejecting the hypothesis H_0. If the p-value is less than or equal to 0.05, the hypothesis for the proposed factor is rejected

with a confidence level of 95% and above on distinguishing the skill performance between novice and expert surgeons and validating the motion system.

The p-value is derived from a cumulative F-distribution table by using a computed $f-value$. The F-distribution table is given in most Statistics text books or installed in most statistics software. The computed $f-value$ is derived as follows:

1. $\mu = \frac{1}{k}\sum_{i=1}^{k}\mu_i$, where k is equal to 2 which refers to two different groups; thus, $i \in \{J, E\}$.
2. Factor sum of squares: $\text{SSA} = N_i\sum_{i=1}^{k}(\mu_i - \mu)^2$, where N_i refers to the number of sample of points in the respective group.
3. Error sum of squares: $\text{SSE} = \sum_{i=1}^{k}\sum_{j=1}^{N_i}(x_{ij} - \mu_i)^2$.
4. $\text{s}_1^2 = \frac{\text{SSA}}{k-1}$
5. $\text{s}^2 = \frac{\text{SSE}}{k(N_i - 1)}$
6. $f-value = \frac{\text{s}_1^2}{\text{s}^2}$

The ANOVA1 function built in MATLAB®'s Statistics Toolbox is used to test the hypothesis: the function returns the p-value and box-and-whisker plot with notches on or off. The box plot is described detailed in the next section.

3.4.1 Box-and-Whisker Plot

As depicted in Figure 3.2, the box plot shows the distribution of the input data: percentiles, three quartiles (Q1, Q2 and Q3), interquartile range (IQR), and outliers. It can be explained as follows:

1. Data in each group are arranged from maximum to minimum values
2. The P-th percentile(P) for the data is obtained by the following steps (Schoonjans *et al.*, 2011):
   (a) Calculate the rank: $r = \frac{1}{2} + \frac{P.N_i}{100}$ where N_i refers to the number of data points
   (b) Round the rank(r) into the nearest integer and take the data value corresponding from the rank

3. The quartiles separate the data into four sessions:

   (a) Q2 is the median value and it divides the data into two halves: lower half and higher half. It is the 50th percentile of the data.

   (b) Q1 is the median value of the lower half of data: it is the 25th percentile of the data, which separates the lower quarter of the data from the rest.

   (c) Q3 is the median value of the higher half of data: it is the 75th percentile of the data, which separates the upper quarter of the data from the rest.

4. IQR = Q3 - Q1 which can be used as a measure of how the data are spread out

5. The outliers are the minimum and maximum values

As depicted in Figure 3.3, the notches in the box plot indicate the approximate confidence intervals around the medians. The notches are calculated as $\frac{Q2+/-(1.57\ .\ IQR)}{\sqrt{N_i}}$ (Chambers, 1983). The box plot with the notches are used when the sample range is large. If two boxes notches from different groups do not overlap, the proposed factor is rejected with a confidence level of 95% and above.

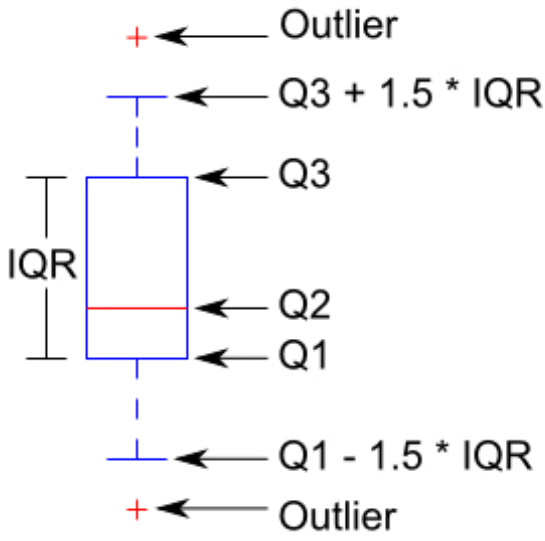

Figure 3.2: Box Plot

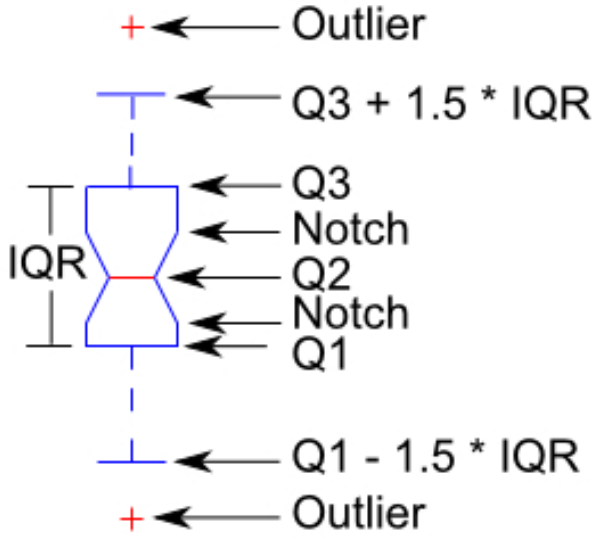

Figure 3.3: Box Plot with Notches

3.5 Results

As depicted in Figures 3.4 – 3.14, the null hypotheses for the respective measurements can be rejected because the corresponding p-values are all less than or equal to 0.05. Therefore, these factors are proved to statistically distinguish the skill performance between novice and expert surgeons. Consequently the Ascension 3DGuidance trakSTAR system for tracking the tip movements of laparoscopic tools is validated.

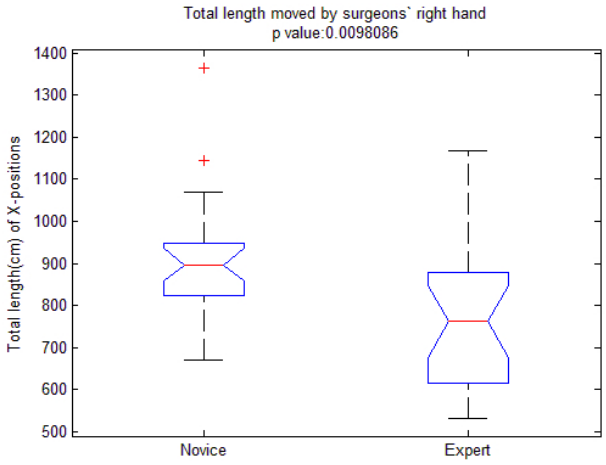

Figure 3.4: Range of the total length moved by novices' right hand along the x-axis is from 670 cm to 1360 cm whereas the range of the total length moved by experts' right hand is from 530 cm to 1170 cm.

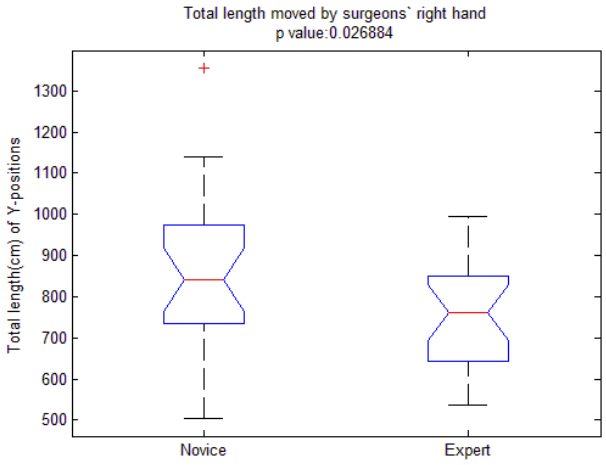

Figure 3.5: Range of the total length moved by novices' right hand along the y-axis is from 500 cm to 1360 cm whereas the range of the total length moved by experts' right hand is from 535 cm to 1000 cm.

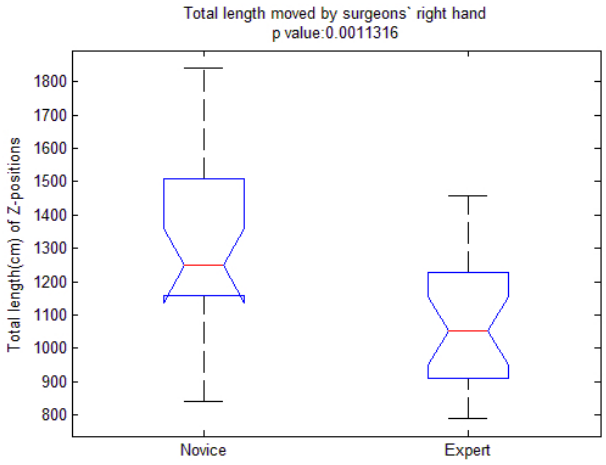

Figure 3.6: Range of the total length moved by novices' right hand along the z-axis is from 840 cm to 1840 cm whereas the range of the total length moved by experts' right hand is from 790 cm to 1460 cm.

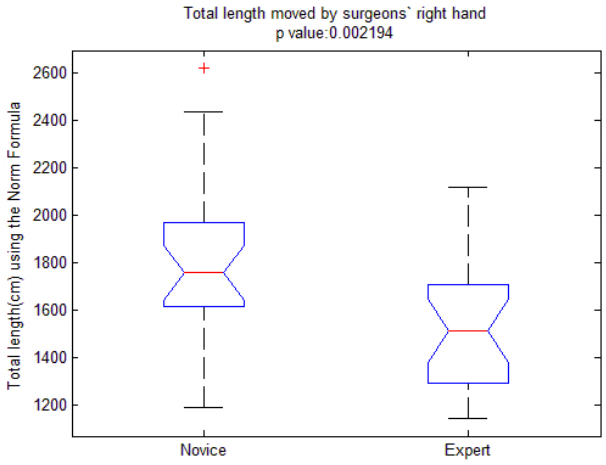

Figure 3.7: Range of the total length moved by novices' right hand using the norm formula is from 1190 cm to 2620 cm whereas the range of the total length moved by experts' right hand is from 1140 cm to 2120 cm.

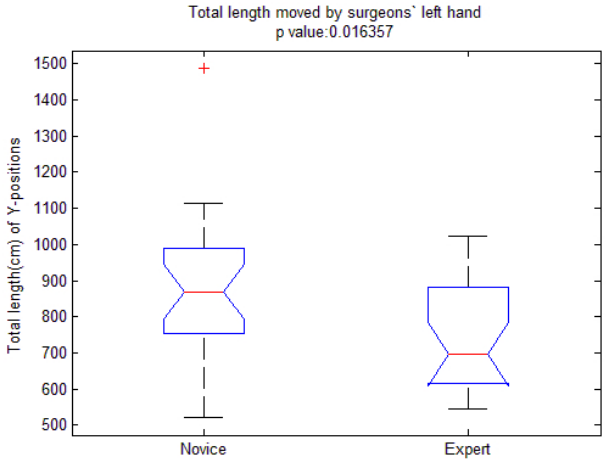

Figure 3.8: Range of the total length moved by novices' left hand along the y-axis is from 520 cm to 1490 cm whereas the range of the total length moved by experts' left hand is from 550 cm to 1020 cm.

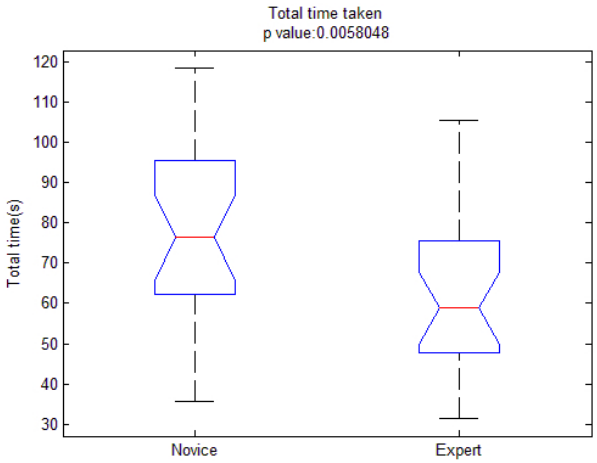

Figure 3.9: Range of the total time taken by novices is from 36 s to 118 s whereas the range of the total time taken by experts is from 31 s to 105 s.

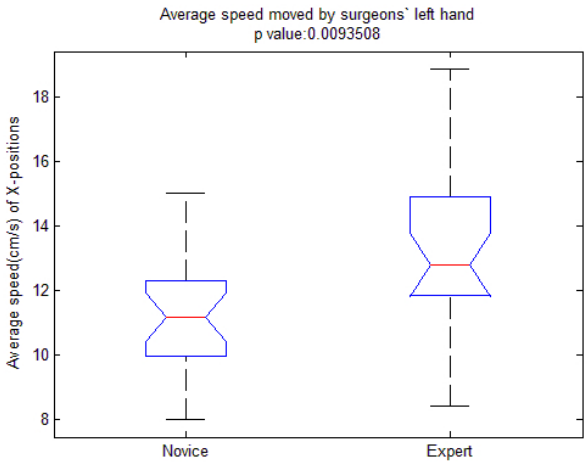

Figure 3.10: Range of the average speed moved by novices' left hand along the x-axis is from 8 cm/s to 15 cm/s whereas the range of the average speed moved by experts' left hand is from 8 cm/s to 19 cm/s.

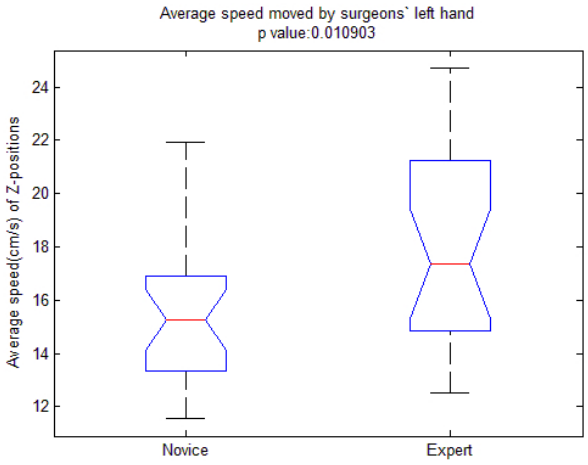

Figure 3.11: Range of the average speed moved by novices' left hand along the z-axis is from 12 cm/s to 22 cm/s whereas the range of the average speed moved by experts' left hand is from 13 cm/s to 25 cm/s.

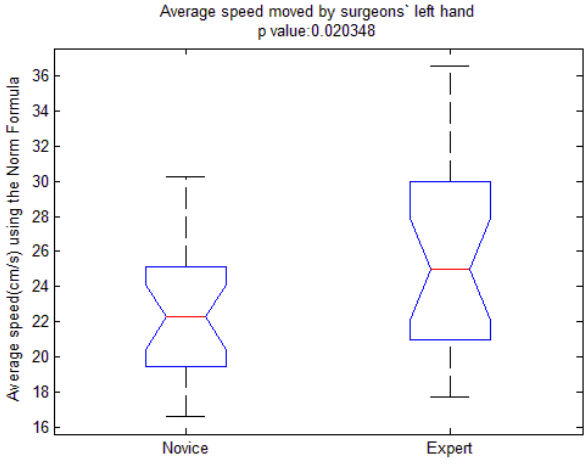

Figure 3.12: Range of the average speed moved by novices' left hand using the norm formula is from 17 cm/s to 30 cm/s whereas the range of the average speed moved by experts' left hand is from 18 cm/s to 37 cm/s.

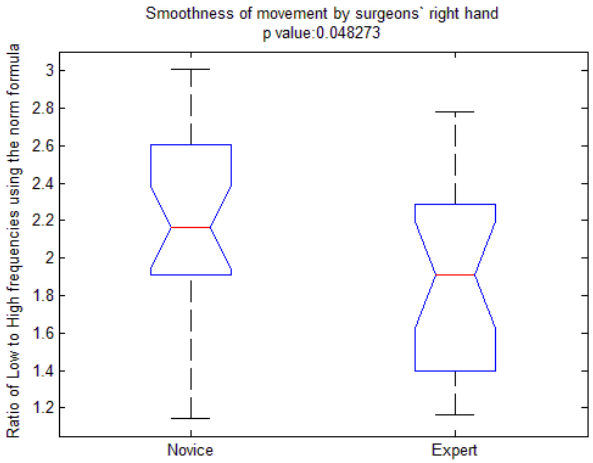

Figure 3.13: Range of the smoothness of movement by novices' right hand using the norm formula is from 1.1 to 3.0 whereas the range of the smoothness of movement by experts' right hand is from 1.2 to 2.8.

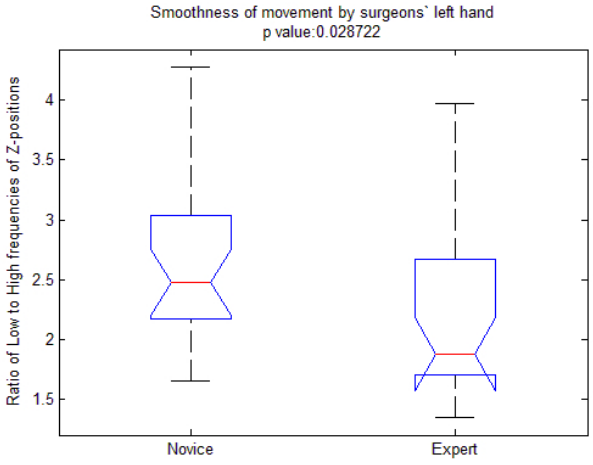

Figure 3.14: Range of the smoothness of movement by novices' left hand along the z-axis is from 1.7 to 4.3 whereas the range of the smoothness of movement by experts' left hand is from 1.4 to 3.9.

3.6 Metric Scales using the Results from the Statistical Method

As mentioned in the hypotheses testing section, the lowest p-value indicates the highest confidence level of rejecting the hypothesis. The hypothesis tests mentioned in the statistical method proved that the following factors have the lowest p-value in each category:

- the path length moved by surgeons' right hands along the z-axis
- the total time taken by surgeons
- the average speed of the surgeons' left hands along the x-axis
- the smoothness of the movement of the surgeons' left hands along the z-axis

The metric scales on the skill performance of surgeons are obtained by using a regression procedure to find the weights of these four factors. All these factor measurements in each category are first normalized so that all the measured values range from lower to higher rates. The lowest rate, which is equal to zero, represents the poorest skill performance and the highest rate, which is equal to 100, represents the best skill performance. The normalized constant values are saved into a vector $\mathbf{nv} = \{nv_1, nv_2, nv_3, nv_4\}$ for future analysis.

These normalized factor measurements are used to fill matrix, M_{Stat} where $M_{\text{Stat}} \in \Re^{m \times n}$, where $m = 48 = 16$ surgeons $\times$ 3 trials and $n = 4$ factors as indicated above. Then, the metric scores for all surgeons are initialized objectively and used to fill a vector, $\mathbf{s}_{\text{Stat}}$: the elements of the vector $\mathbf{s}_{\text{Stat}}$ is assigned the value 100 if the corresponding surgeon is an expert and a value 1 if a novice. The weights of these four factors are obtained by regressing the input matrix M_{Stat} onto the vector $\mathbf{s}_{\text{Stat}}$. Algorithm 1 outlines the method to obtain the weights of these four factors. The weights are inversely related to the p-values. Thus, these weights are directly related to the confidence level for rejecting the above proposed hypotheses. Each surgeon's skill performance is scored by multiplying the input four factors,$\mathbf{f}$, with weights,$\mathbf{w}$, which are the output from Algorithm 1. Using Formula 3.2, the competency-based score for a surgeon is achieved. Figure 3.15 shows the scores that are achieved by all surgeons while performing three trials of the peg transfer task. The scores were better for more experienced surgeons. The Matlab software provided by Michael Grant and Stephen Boyd is used to find the weights (Grant and Boyd, 2013).

$$\underset{\mathbf{w}}{\text{minimize}} \quad ||\mathrm{M}_{\mathrm{Stat}}\mathbf{w} - \mathbf{s}_{\mathrm{Stat}}||_2^2 \tag{3.1}$$

Algorithm 1 Find the weights of four factors

Input: $\mathrm{M}_{\mathrm{Stat}}$
Output: $\mathbf{w} = \{w_1, w_2, w_3, w_4\}$
1: $\mathbf{w} \leftarrow$ Equation 3.1
2: $\mathrm{Sum}_w \leftarrow$ Sum the elements of $\mathbf{w}$
3: $\mathbf{w} \leftarrow$ Divide each element of w by Sum_w so that $||\mathbf{w}||_1 = 1$

$$\begin{aligned} \mathbf{f}_{\mathrm{new}} &=< f1/nv1, f2/nv2, f3/nv3, f4/nv4 > \\ \mathrm{MetricScale} &= \mathbf{f}_{\mathrm{new}} \cdot \mathbf{w}' \end{aligned} \tag{3.2}$$

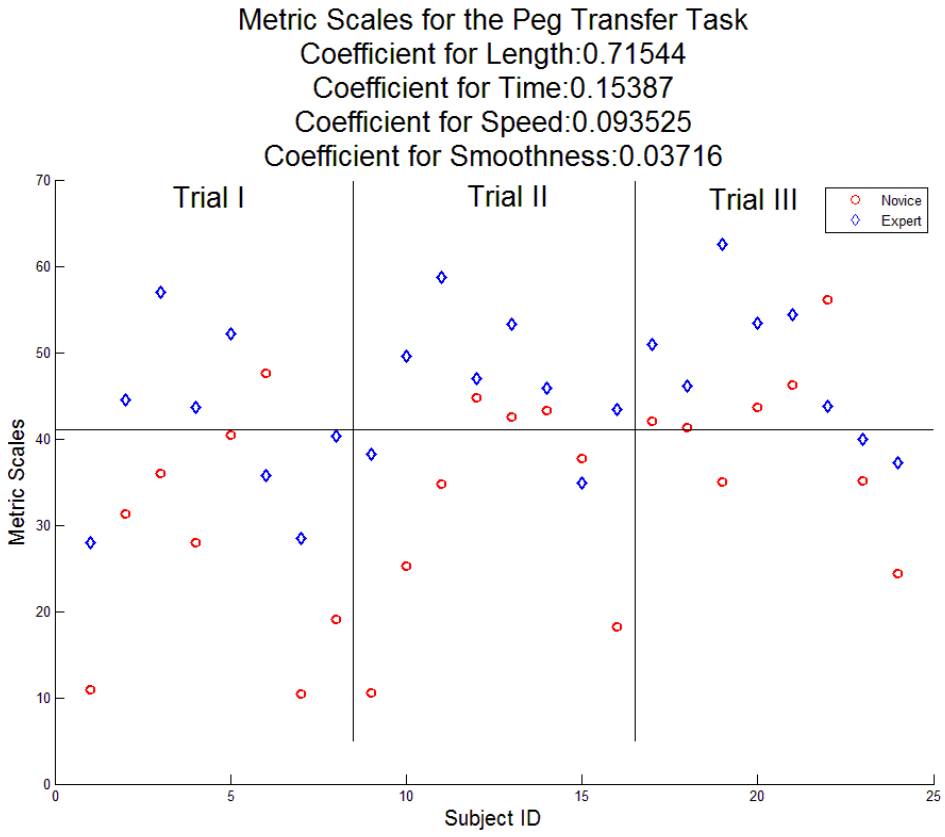

Figure 3.15: Metric Scales for the Peg Transfer Task

Chapter 4

Machine Learning Approach and Results

The machine learning approach predicts whether a recorded trajectory is performed by a novice or an expert. As depicted in Figure 4.1, it includes five steps: hand trajectory segmentation, feature extraction, feature selection, classification and evaluation. Hand trajectory segmentation in the machine learning approach segments the laparoscopic tip movements into different stages: reach, lift, transport and release of pegs. Similar to the statistical approach, features that may contribute to the skill performance between novice and expert surgeons are defined. These features with m samples are arranged in a matrix format; mathematically, $A \in \Re^{m \times n}$, where m stands for the number of training samples and n stands for input features. There is also a label vector that includes $+1$ which represents the skill performance of a novice surgeon and -1 which represents the skill performance of an expert surgeon. The best features, which are the most statistically related to the labels, are selected by using either principal component analysis (PCA) or minimum redundancy and maximum relevance feature selection(mRMR) (Wang and Summers, 2012). The classifier finds the relationship between the selected features and a label. Two classifiers, namely, the Fisher linear discriminant (FLD) and the support vector machine (SVM), are introduced. Each classifier is combined with any feature selection method resulting in four models for predicting surgeon skill performance:

1. PCA feature selection with FLD classifier
2. PCA feature selection with SVM classifier
3. mRMR feature selection with FLD classifier
4. mRMR feature selection with SVM classifier

The overall performance of these four models is evaluated by using leave-one-out cross validation method (Khodayari-Rostamabad *et al.*, 2013).

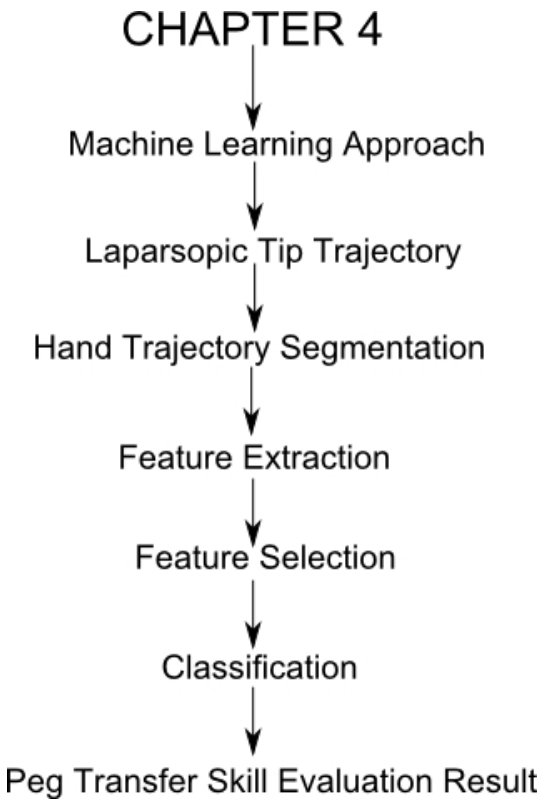

Figure 4.1: Chapter 4 Outline

4.1 Hand Trajectory Segmentation

Hand trajectory segmentation is achieved by detecting different positions of pegs and the changes in the velocity of each hand movement (Flanagan *et al.*, 2006). It is segmented into different stages: reach, lift, transport and release.

As depicted in Figure 4.2 and Figure 4.3, the first peg chosen is located at the minimum x values, which are the closest to the transmitter, and the last peg chosen is located at the maximum x values, which are the furthest from the transmitter. The negative y-positions indicate the grasper at the left side of the transmitter, and the positive y-positions indicate the grasper at the right side of the transmitter as depicted in Figure 4.4 and Figure 4.5. The minimum z-positions are at the pick-up regions, and the maximum z-positions are at the transferring regions as depicted in Figure 4.6 and Figure 4.7. Thus, different positions of each peg in the x and z axis are mainly used in the segmentation. When the grasper is moved from mid-air to the peg position, a negative velocity in the z-axis is observed. When the grasper is moved from the peg position to mid-air, a positive velocity in the z-axis is observed. While picking up or transferring the peg, there is a pause that indicates zero velocity. Thus, different directions of the velocity in the z-axis are also used in the segmentation. All data are sampled at 60 Hz.

Hand trajectory segmentation is achieved by two steps:

1. Partition the Task into Two Segments
2. Segmentation of Individual Peg Movements

The following subsections describe the details of each step.

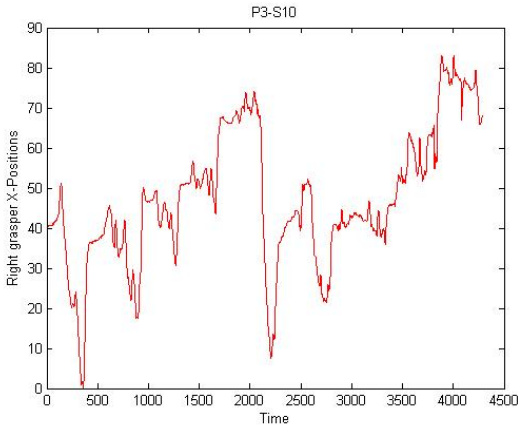

Figure 4.2: Right Grasper X-positions

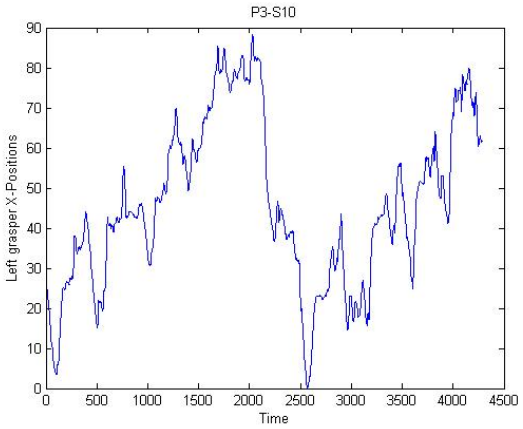

Figure 4.3: Left Grasper X-positions

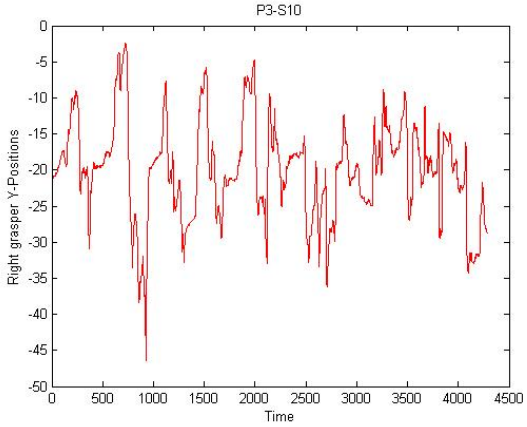

Figure 4.4: Right Grasper Y-positions

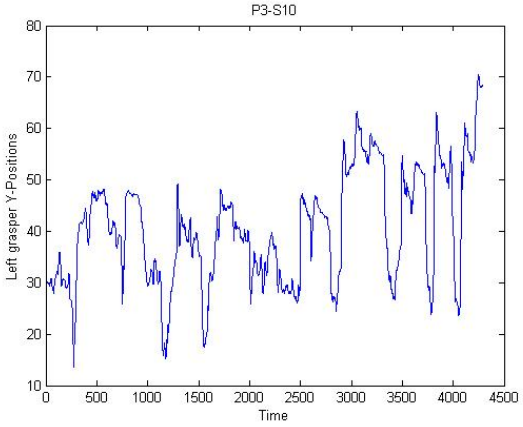

Figure 4.5: Left Grasper Y-positions

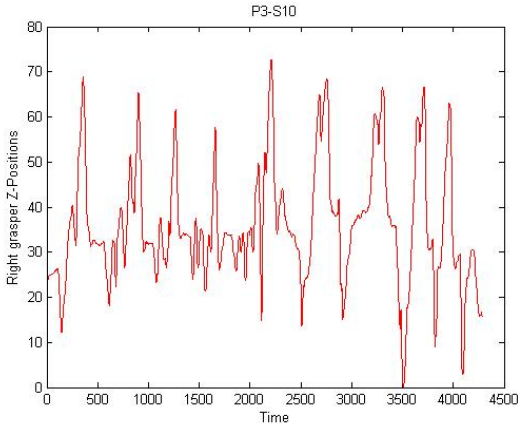

Figure 4.6: Right Grasper Z-positions

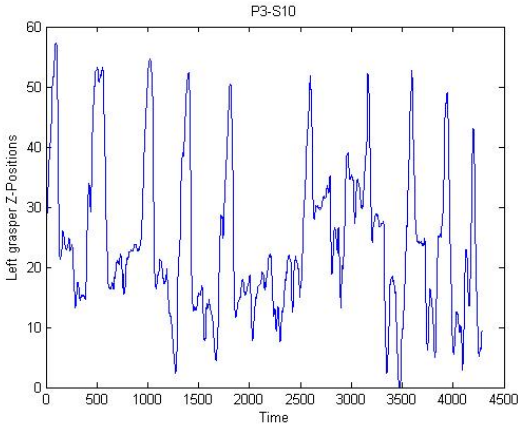

Figure 4.7: Left Grasper Z-positions

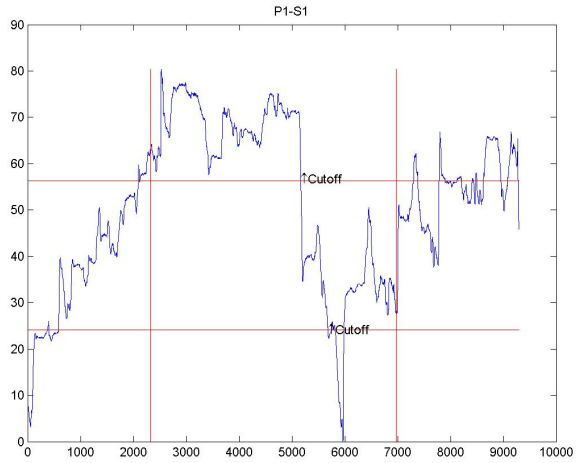

Figure 4.8: Partition the task into two segments

4.1.1 Partition the Task into Two Segments

As mentioned in Chapter 2, five pegs were placed on the pegboard on the surgeon's left side and arranged in the order of nearest to furthest with respect to the transmitter. After all five pegs from the left side were picked and placed to the right side, these five pegs were moved back to surgeon's left side in the same order. When a surgeon switched picking from the left side to right side, swift movements in the x-axis and z-axis are detected. Because swift movements could contribute to high frequency component noise, the trajectory is partitioned into two segments.

The last peg dropped from the left side was located furthest from the transmitter and the first peg picked from the right side was located closest to the transmitter. As depicted in Figure 4.8, the furthest positions from the transmitter refer to the maximum values and the closest positions to the transmitter refer to the minimum values in the trajectory. Therefore, partitioning the task into two segments is achieved by detecting the transition from the maximum value to the minimum value in the trajectory. This transition should not be detected within a 25% interval from the start and from the end of the trajectory. Figure 4.8 also highlights these facts and Algorithm 2 outlines the method. The last peg picked form the left side is denoted as t_{DLR} and the first peg picked from the right side is denoted as t_{PFL} in the algorithm. The input vector $\mathbf{x}$ constitutes the time series of the trajectory of the grasper in surgeon's right hand along the x-axis. All data are sampled at 60 Hz.

Algorithm 2 Look for t_{DLR} and t_{PFL}

Input: x=$\{x_1, x_2, x_3, ..., x_N\}$
Output: t_{DLR}, t_{PFL}

$t_{DLR} \leftarrow N$
$t_{PFL} \leftarrow 0$
lim $\leftarrow$0.25
while t_{DLR} >t_{PFL} **do**
  $t_{Ulim} \leftarrow$ T - (T $\cdot$ lim)
  $t_{Llim} \leftarrow$ T $\cdot$ lim
  MX $\leftarrow 0$
  for $i = t_{Llim}$ **to** t_{Ulim} **do**
    if MX $< x_i$ **then**
      MX $\leftarrow x_i$
    end if
  end for
  MN $\leftarrow$ MX
  for $i = t_{Llim}$ **to** t_{Ulim} **do**
    if MN $> x_i$ **then**
      MN $\leftarrow x_i$
    end if
  end for
  $POS_{mx} \leftarrow$ MX $-$ (MX $\cdot$ 0.3)
  $POS_{mn} \leftarrow$ MN $+$ (MN $\cdot$ 0.3)
  for $i = t_{Llim}$ **to** t_{Ulim} **do**
    if $x_i \leq POS_{mn}$ **then**
      $t_{PFL} \leftarrow i$
      break
    end if
  end for
  for $i = t_{Ulim}$ **downto** t_{Llim} **do**
    if $x_i \geq POS_{mx}$ **then**
      $t_{DLR} \leftarrow i$
      break
    end if
  end for
  if $t_{DLR} > t_{PFL}$ **then**
    $lim \leftarrow lim + 0.1$
  end if
end while

4.1.2 Segmentation of Individual Peg Movements

The extracted trajectory from the previous section is further used to segment the path from picking a peg to transferring this peg. Then, the extracted trajectory is filtered to remove high-frequency components by a third-order Butterworth filter with the cut-off frequency of three Hz, and then it is smoothed by the cross-correlation with a Gaussian pulse with the variance of three. Then, the velocity, which is defined as the rate of change of measurements between any two consecutive sample points, is used to identify the path for picking or dropping a peg, and the path for transferring a peg to another hand. The path of picking or dropping a peg is obtained by grouping all the consecutive negative signs of the velocities. Similarly, the path of transferring a peg is obtained by grouping all the consecutive positive signs of the velocities. The zero velocities indicate steady-state picking, dropping and transferring pegs. Algorithm 3 outlines the method and the following figures show the steps for segmenting the path of an individual peg movement.

Algorithm 3 Look for $\mathbf{t}$

Input: $\mathbf{z}=\{z_1, z_2, z_3, ..., z_{\mathrm{NR}}\}$
Output: $\mathbf{t}$

1: $\mathbf{z}_{\mathrm{F}} \leftarrow$ Filtered input $\mathbf{z}$ by third order butter worth filter
2: $\mathbf{z}_{\mathrm{S}} \leftarrow$ Smooth filtered output $\mathbf{z}_{\mathrm{F}}$ by cross-correlation with Gaussian pulse
3: $\mathbf{z}_{\mathrm{Rec}} \leftarrow$ Downsample $\mathbf{z}_{\mathrm{S}}$ by 10-fold
4: $\mathbf{z}_{\mathrm{vel}} \leftarrow$ A set of velocities calculating from $\mathbf{z}_{\mathrm{Rec}}$
5: $\mathbf{t}_{\mathrm{neg}} \leftarrow$ negative slope start points from $\mathbf{z}_{\mathrm{vel}}$
6: $\mathbf{t}_{\mathrm{pos}} \leftarrow$ positive slope start points from $\mathbf{z}_{\mathrm{vel}}$
7: $\mathbf{t}_{\mathrm{tzvel}} \leftarrow$ index of lowest z values between $\mathbf{t}_{\mathrm{neg}}$ and $\mathbf{t}_{\mathrm{pos}}$
8: $\mathbf{t}_{\mathrm{th}} \leftarrow$ index of z values which are lower than the threshold value in $\mathbf{t}_{\mathrm{tzvel}}$
9: $\mathbf{t} \leftarrow$ index of the positive slope which is higher than the threshold value in $\mathbf{t}_{\mathrm{th}}$

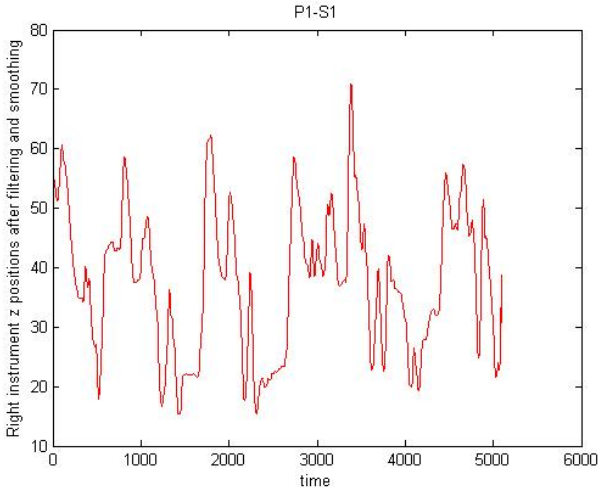

Figure 4.9: Filtered high-frequency components and smoothed data

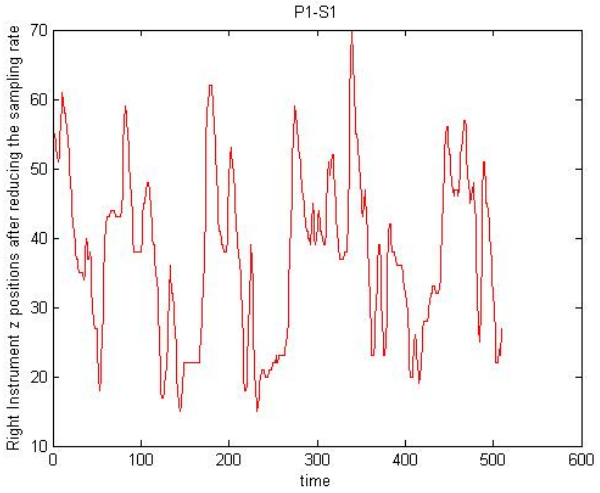

Figure 4.10: Reduce Sampling Rate

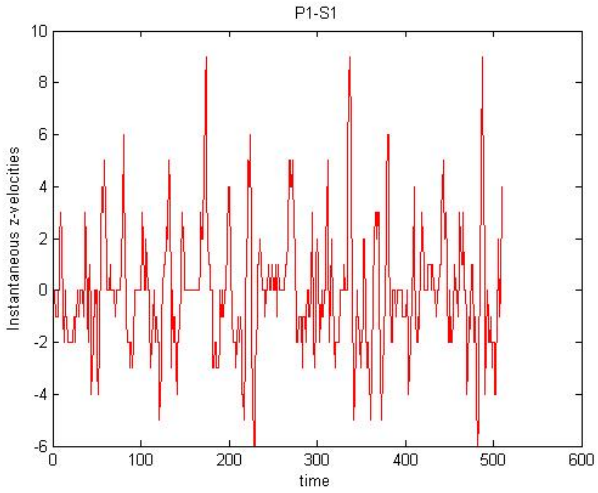

Figure 4.11: z-velocities

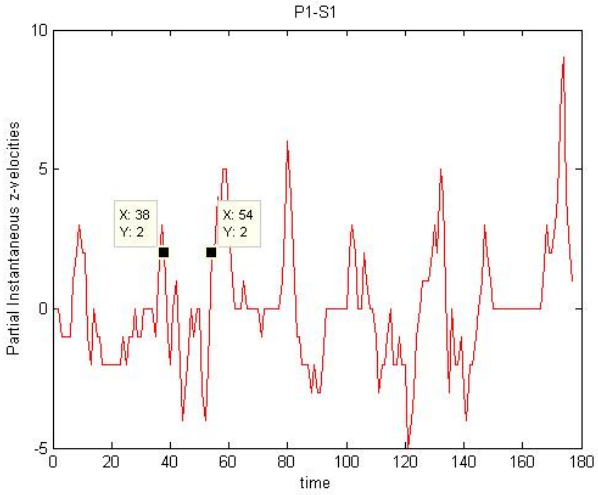

Figure 4.12: Interval of negative z-velocity start and end

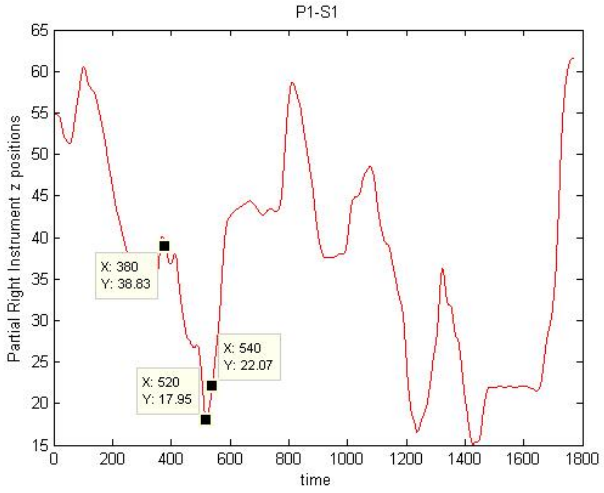

Figure 4.13: Z minimum point within the interval of negative z-velocity start and end

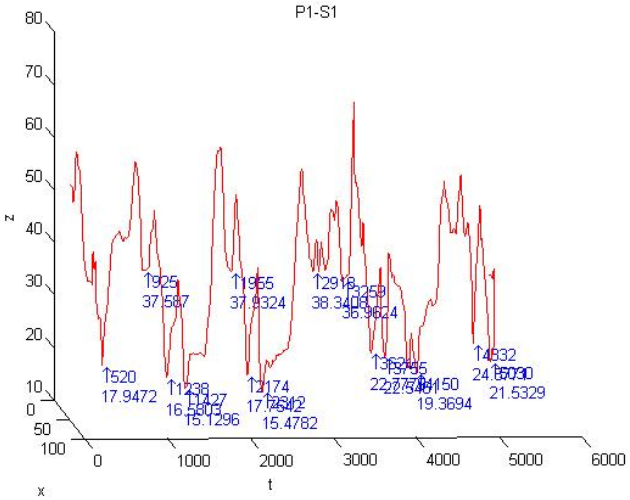

Figure 4.14: All Features Extracted

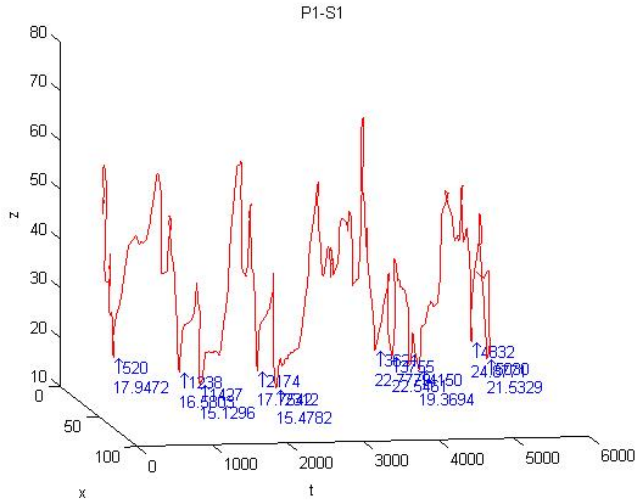

Figure 4.15: Extract Features below z threshold

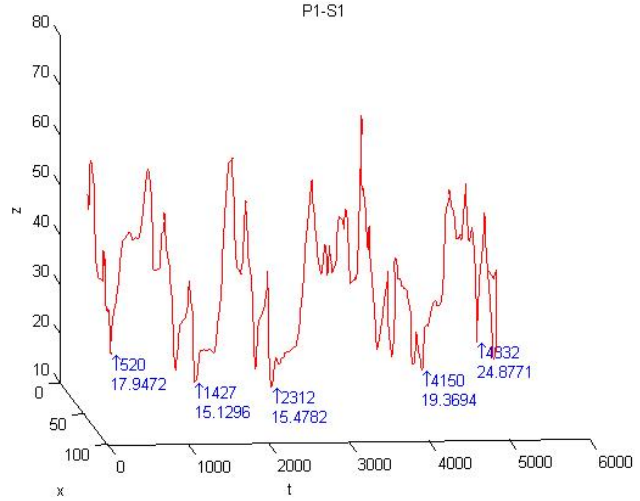

Figure 4.16: Extract Features whose positive slopes are above threshold

4.2 Feature Extraction

Similar to the statistical approach mentioned in Chapter 3, path length, time, average speed and smoothness features are extracted for the measurement of economy, efficiency and hand tremor. All these features are also further grouped into measurements along the x-axis, y-axis, and z-axis and measurements using the norm formula.

Using the time index outputs from Algorithm 2, the measurement features for path length, time, the average speed and smoothness are further grouped into the following:

- Picking all pegs from a surgeon's right to left side
- Dropping all pegs from a surgeon's right to left side
- Picking all pegs from a surgeon's left to right side
- Dropping all pegs from a surgeon's left to right side

Using the same steps from line 1 to line 7 of Algorithm 3, the number of up and down movement features for the measurement of economy are also extracted. There are 74 features in total and Tables 4.1 – 4.5 describe the details of each feature.

Table 4.1: Time Features

Description	Symbol	Definition	Justification	Unit
Duration from the first peg picked to the last peg dropped	T_{whole}	$T_{DL5} - T_{PR1}$	Efficiency	second
Duration of moving all five pegs from surgeon's right to left side	T_{RL}	$T_{DR5} - T_{PR1}$	Efficiency	second
Duration of moving all five pegs from surgeon's left to right side	T_{LR}	$T_{DL5} - T_{PL1}$	Efficiency	second
Duration of switching between surgeon's right side and left side	T_S	$T_{whole} - T_{RL} - T_{LR}$	Efficiency	second

Table 4.2: Length Features

Description	Symbol	Definition	Justification	Unit
Total length moved by surgeon's right hand	L_{xr}	$\sum_{i=t_{PFR}}^{t_{DLL}-1} \lvert x_i - x_{i+1} \rvert$	Economy	centimetre
	L_{yr}	$\sum_{i=t_{PFR}}^{t_{DLL}-1} \lvert y_i - y_{i+1} \rvert$		
	L_{zr}	$\sum_{i=t_{PFR}}^{t_{DLL}-1} \lvert z_i - z_{i+1} \rvert$		
	L_{nr}	$\sqrt{L_{xr}^2 + L_{yr}^2 + L_{zr}^2}$		
Total length moved by surgeon's left hand	L_{xl}	$\sum_{i=t_{DFR}}^{t_{PLL}-1} \lvert x_i - x_{i+1} \rvert$	Economy	centimetre
	L_{yl}	$\sum_{i=t_{DFR}}^{t_{PLL}-1} \lvert y_i - y_{i+1} \rvert$		
	L_{zl}	$\sum_{i=t_{DFR}}^{t_{PLL}-1} \lvert z_i - z_{i+1} \rvert$		
	L_{nl}	$\sqrt{L_{xl}^2 + L_{yl}^2 + L_{zl}^2}$		
Total length moved while picking five pegs from surgeon's right to left side	L_{pxrl}	$\sum_{i=t_{PFR}}^{t_{PLR}-1} \lvert x_i - x_{i+1} \rvert$	Economy	centimetre
	L_{pyrl}	$\sum_{i=t_{PFR}}^{t_{PLR}-1} \lvert y_i - y_{i+1} \rvert$		
	L_{pzrl}	$\sum_{i=t_{PFR}}^{t_{PLR}-1} \lvert z_i - z_{i+1} \rvert$		
	L_{pnrl}	$\sqrt{L_{pxrl}^2 + L_{pyrl}^2 + L_{pzrl}^2}$		
Total length moved while dropping five pegs from surgeon's right to left side	L_{dxrl}	$\sum_{i=t_{DFR}}^{t_{DLR}-1} \lvert x_i - x_{i+1} \rvert$	Economy	centimetre
	L_{dyrl}	$\sum_{i=t_{DFR}}^{t_{DLR}-1} \lvert y_i - y_{i+1} \rvert$		
	L_{dzrl}	$\sum_{i=t_{DFR}}^{t_{DLR}-1} \lvert z_i - z_{i+1} \rvert$		
	L_{dnrl}	$\sqrt{L_{dxrl}^2 + L_{dyrl}^2 + L_{dzrl}^2}$		
Total length moved while picking five pegs from surgeon's left to right side	L_{pxlr}	$\sum_{i=t_{PFL}}^{t_{PLL}-1} \lvert x_i - x_{i+1} \rvert$	Economy	centimetre
	L_{pylr}	$\sum_{i=t_{PFL}}^{t_{PLL}-1} \lvert y_i - y_{i+1} \rvert$		
	L_{pzlr}	$\sum_{i=t_{PFL}}^{t_{PLL}-1} \lvert z_i - z_{i+1} \rvert$		
	L_{pnlr}	$\sqrt{L_{pxlr}^2 + L_{pylr}^2 + L_{pzlr}^2}$		
Total length moved while dropping five pegs from surgeon's left to right side	L_{dxlr}	$\sum_{i=t_{DFL}}^{t_{DLL}-1} \lvert x_i - x_{i+1} \rvert$	Economy	centimetre
	L_{dylr}	$\sum_{i=t_{DFL}}^{t_{DLL}-1} \lvert y_i - y_{i+1} \rvert$		
	L_{dzlr}	$\sum_{i=t_{DFL}}^{t_{DLL}-1} \lvert z_i - z_{i+1} \rvert$		
	L_{dnlr}	$\sqrt{L_{dxlr}^2 + L_{dylr}^2 + L_{dzlr}^2}$		

Table 4.3: Average Speed Features

Description	Symbol	Definition	Justification	Unit
Average speed moved by surgeon's right hand	Sp_{xr}	$\frac{L_{xr}}{t_{DLL}-t_{PFR}}$	Efficiency	$\frac{\text{centimetre}}{\text{second}}$
	Sp_{yr}	$\frac{L_{yr}}{t_{DLL}-t_{PFR}}$		
	Sp_{zr}	$\frac{L_{zr}}{t_{DLL}-t_{PFR}}$		
	Sp_{nr}	$\frac{L_{nr}}{t_{DLL}-t_{PFR}}$		
Average speed moved by surgeon's left hand	Sp_{xl}	$\frac{L_{xl}}{t_{PLL}-t_{DFR}}$	Efficiency	$\frac{\text{centimetre}}{\text{second}}$
	Sp_{yl}	$\frac{L_{yl}}{t_{PLL}-t_{DFR}}$		
	Sp_{zl}	$\frac{L_{zl}}{t_{PLL}-t_{DFR}}$		
	Sp_{nl}	$\frac{L_{nl}}{t_{PLL}-t_{DFR}}$		
Average speed moved while picking five pegs from surgeon's right to left side	Sp_{pxrl}	$\frac{L_{pxrl}}{t_{PLR}-t_{PFR}}$	Efficiency	$\frac{\text{centimetre}}{\text{second}}$
	Sp_{pyrl}	$\frac{L_{pyrl}}{t_{PLR}-t_{PFR}}$		
	Sp_{pzrl}	$\frac{L\vert_{pzrl}}{t_{PLR}-t_{PFR}}$		
	Sp_{pnrl}	$\frac{L_{pnrl}}{t_{PLR}-t_{PFR}}$		
Average speed moved while dropping five pegs from surgeon's right to left side	Sp_{dxrl}	$\frac{L_{dxrl}}{t_{DLR}-t_{DFR}}$	Efficiency	$\frac{\text{centimetre}}{\text{second}}$
	Sp_{dyrl}	$\frac{L_{dyrl}}{t_{DLR}-t_{DFR}}$		
	Sp_{dzrl}	$\frac{L_{dzrl}}{t_{DLR}-t_{DFR}}$		
	Sp_{dnrl}	$\frac{L_{dnrl}}{t_{DLR}-t_{DFR}}$		
Average speed moved while picking five pegs from surgeon's left to right side	Sp_{pxlr}	$\frac{L_{pxlr}}{t_{PLL}-t_{PFL}}$	Efficiency	$\frac{\text{centimetre}}{\text{second}}$
	Sp_{pylr}	$\frac{L_{pylr}}{t_{PLL}-t_{PFL}}$		
	Sp_{pzlr}	$\frac{L_{pzlr}}{t_{PLL}-t_{PFL}}$		
	Sp_{pnlr}	$\frac{L_{pnlr}}{t_{PLL}-t_{PFL}}$		
Average speed moved while dropping five pegs from surgeon's left to right side	Sp_{dxlr}	$\frac{L_{dxlr}}{t_{DLL}-t_{DFL}}$	Efficiency	$\frac{\text{centimetre}}{\text{second}}$
	Sp_{dylr}	$\frac{L_{dylr}}{t_{DLL}-t_{DFL}}$		
	Sp_{dzlr}	$\frac{L_{dzlr}}{t_{DLL}-t_{DFL}}$		
	Sp_{dnlr}	$\frac{L_{dnlr}}{t_{DLL}-t_{DFL}}$		

Table 4.4: Number of Up and Down Features

Description	Symbol	Definition	Justification	Unit
Number of up and down movements by surgeon's right hand	NUDr NUDrp NUDrd	From Line 1 to Line 7 of Algorithm 3	Economy	unitless
Number of up and down movements by the surgeon's left hand	NUDl NUDlp NUDld	From Line 1 to Line 7 of Algorithm 3	Economy	unitless

Table 4.5: Smoothness Features

Description	Symbol	Definition	Justification	Unit
Smoothness of movement by surgeon's right hand	$\mathrm{Sm}_{\mathrm{pxrl}}$	$\frac{\mathrm{LF}_{\mathrm{pxrl}}}{\mathrm{HF}_{\mathrm{pxrl}}}$	Hand tremor	unitless
	$\mathrm{Sm}_{\mathrm{dxlr}}$	$\frac{\mathrm{LF}_{\mathrm{dxlr}}}{\mathrm{HF}_{\mathrm{dxlr}}}$		
	$\mathrm{Sm}_{\mathrm{pyrl}}$	$\frac{\mathrm{LF}_{\mathrm{pyrl}}}{\mathrm{HF}_{\mathrm{pyrl}}}$		
	$\mathrm{Sm}_{\mathrm{dylr}}$	$\frac{\mathrm{LF}_{\mathrm{dylr}}}{\mathrm{HF}_{\mathrm{dylr}}}$		
	$\mathrm{Sm}_{\mathrm{pzrl}}$	$\frac{\mathrm{LF}_{\mathrm{pzrl}}}{\mathrm{HF}_{\mathrm{pzrl}}}$		
	$\mathrm{Sm}_{\mathrm{dzlr}}$	$\frac{\mathrm{LF}_{\mathrm{dzlr}}}{\mathrm{HF}_{\mathrm{dzlr}}}$		
	$\mathrm{Sm}_{\mathrm{pnrl}}$	$\frac{\mathrm{LF}_{\mathrm{pnrl}}}{\mathrm{HF}_{\mathrm{pnrl}}}$		
	$\mathrm{Sm}_{\mathrm{dnlr}}$	$\frac{\mathrm{LF}_{\mathrm{dnlr}}}{\mathrm{HF}_{\mathrm{dnlr}}}$		
Smoothness of movement by surgeon's left hand	$\mathrm{Sm}_{\mathrm{pxlr}}$	$\frac{\mathrm{LF}_{\mathrm{pxlr}}}{\mathrm{HF}_{\mathrm{pxlr}}}$	Hand tremor	unitless
	$\mathrm{Sm}_{\mathrm{dxrl}}$	$\frac{\mathrm{LF}_{\mathrm{dxrl}}}{\mathrm{HF}_{\mathrm{dxrl}}}$		
	$\mathrm{Sm}_{\mathrm{pylr}}$	$\frac{\mathrm{LF}_{\mathrm{pylr}}}{\mathrm{HF}_{\mathrm{pylr}}}$		
	$\mathrm{Sm}_{\mathrm{dyrl}}$	$\frac{\mathrm{LF}_{\mathrm{dyrl}}}{\mathrm{HF}_{\mathrm{dyrl}}}$		
	$\mathrm{Sm}_{\mathrm{pzlr}}$	$\frac{\mathrm{LF}_{\mathrm{pzlr}}}{\mathrm{HF}_{\mathrm{pzlr}}}$		
	$\mathrm{Sm}_{\mathrm{dzrl}}$	$\frac{\mathrm{LF}_{\mathrm{dzrl}}}{\mathrm{HF}_{\mathrm{dzrl}}}$		
	$\mathrm{Sm}_{\mathrm{pnlr}}$	$\frac{\mathrm{LF}_{\mathrm{pnlr}}}{\mathrm{HF}_{\mathrm{pnlr}}}$		
	$\mathrm{Sm}_{\mathrm{dnrl}}$	$\frac{\mathrm{LF}_{\mathrm{dnrl}}}{\mathrm{HF}_{\mathrm{dnrl}}}$		

4.3 Feature Selection

All measured features from each surgeon are used to fill matrix $A \in \Re^{m \times n}$, where $m = 48 = 16$ surgeons $\times$ 3 trials and $n = 74$ features. These high number of features cause a dimensionality problem, where higher dimensionality results in an unreliable outcome (Theodoridis, 2003). To avoid the dimensionality problem and to save the computational cost, the dimensions of measured features are further reduced by selecting the best features. The best features most statistically dependent on the skill performance between novice and expert surgeons are selected by projecting the data orthogonally onto a lower dimensional linear space (PCA). Alternatively, the best features are selected by measuring the mutual information, the redundancy and the relevant information among features.

In this thesis, because there are 48 samples available, approximately the ratio of one feature to 10 samples is assumed to represent the skill performance of the peg transfers. The exact number is left as future research when there are more data available to analyse.

4.3.1 Principal Component Analysis (PCA)

The PCA is based on the eigenvalue decomposition of the covariance matrix of the data. It finds the linear subspace specified by the orthogonal vectors that form the principal components. The principal components are obtained by collecting the eigenvectors with the large eigenvalues. The large eigenvalues indicate the significance of features in data. All measured features from each surgeon are used to fill matrix $A \in \Re^{m \times n}$ where $m = 48 = 16$ surgeons $\times$ 3 trials and $n = 74$ features. The features of matrix A are further reduced by the following steps:

1. Subtract the average of measurements for all surgeons in each feature from matrix A; the outcome is denoted as A_c, $A_c \in \Re^{m \times n}$.

2. Calculate the covariance matrix of the data, $C = A_c^T A_c$, $where\, C \in \Re^{n \times n}$.

3. Calculate the eigenvectors (V) and eigenvalues of the covariance matrix C, $V \in \Re^{n \times n}$.

4. Choose the eigenvectors that have large eigenvalues. These eigenvectors are known as principal components.

5. Multiply data with the principal components, and then the dimension of A_c is reduced; the outcome is denoted as $A_r = AV_r$, $A_r \in \Re^{m \times r}$, $V_r = \in \Re^{m \times r}$.

6. Save the eigenvectors for subsequent analysis.

If there are fewer observations than features, the computational cost is further reduced by the following steps: If $A \in \Re^{m \times n}$,

1. Subtract the average of measurements for all surgeons in each feature from matrix A; the outcome is denoted as A_c, $A_c \in \Re^{m \times n}$.

2. Calculate the covariance matrix of the data, $C = A_c A_c^T$, $where\, C \in \Re^{m \times m}$.

3. Calculate the eigenvectors (U) and eigenvalues of the covariance matrix C, $where\, U \in \Re^{m \times m}$.

4. Choose the eigenvectors that have the large eigenvalues. If there are r large eigenvalues, the dimension of U becomes $U_r \in \Re^{m \times r}$.

5. Multiply A_c^T with U_r; the outcome is denoted as $U_n = A_c^T U_r$, $where\, U_n \in \Re^{n \times r}$ and divide each element of U_n with the corresponding norm of column vector U_r.

6. Multiply data A_c with the reduced and normalized eigenvectors U_n and then, the dimension of A_c is reduced; the outcome is denoted as $A_r = A_c U_n$, $A_r \in \Re^{m \times r}$.

7. Save the eigenvectors for subsequent analysis.

Result from Principal Component Analysis Feature Selection

Eigenvectors, which have four large eigenvalues, are assumed to represent the skill performance of the peg transfer task.

4.3.2 Minimum Redundancy and Maximum Relevance Feature Selection (mRMR)

Mutual information is a measurement of the statistical relation between two random variables (Ding and Peng, 2005). If the mutual information between two features is zero, it indicates that the two features are independent. If the mutual information is large, the two features are dependent. The

mutual information of two random variables X and Y is defined based on their joint probability distribution p(x,y) and the respective marginal probabilities p(x) and p(y).

$$I(X;Y) = \sum_{i,j} p(x_i, y_j) \log \frac{p(x_i, y_j)}{p(x_i)p(y_j)}$$

Feature dimensions are reduced by minimizing redundancy among features and maximizing the relation between features and the targeted group. Minimizing redundancy among features is obtained by

$$minimize \quad W_I, \quad W_I = \frac{1}{|S|^2} \sum_{i,j \in S} I(i,j),$$

where S is the set of features and $I(i,j)$ is the mutual information between two features.
Maximizing the relation between features and the targeted group is obtained by

$$maximize \quad V_I, \quad V_I = \frac{1}{|S|^2} \sum_{i \in S} I(h,i),$$

where S is the set of features and $I(h,i)$ is the mutual information between the feature and classification label. Thus, the best feature is chosen by optimizing the two above functions. By assuming the two functions are equally important, the formula becomes

$$\max_{i \in \Omega_S} aximize \quad (V_I - W_I), \quad \max_{i \in \Omega_S} \text{imize}[I(i,h) - \frac{1}{|S|} \sum_{j \in S} I(i,j)]$$

Ω is the entire set.

The mRMR programs provided by Dr. Hanchuan Peng is used to select features.
`http://penglab.janelia.org/proj/mRMR/`

Result from the Mutual Information, Minimum Redundancy, and Maximum Relevance Feature Selection

The most relevant four features are selected by leaving out one sample at a time and training the rest of the features. Thus, there are N different combination of the four features. These four features are selected by choosing the most relevant features that occur the most in N different combinations.

They are as follows:

1. Smoothness of movement of the surgeon's right hand along the z-axis while picking all five pegs from the surgeon's right to the left side
2. Smoothness of movement of the surgeon's right hand along the z-axis while dropping all five pegs from the surgeon's left to the right side
3. Smoothness of movement of the surgeon's left hand along the z-axis while dropping all five pegs from the surgeon's right to the left side
4. Total length moved by the surgeon's right hand along the x-axis

4.4 Classification

Because two different groups must be classified, binary classification is used (Statnikov *et al.*, 2011). Binary classification is defined by using a real-valued function $f(\mathbf{x})$ where $\mathbf{x}$ is the selected feature vector $\mathbf{x} = (x_1, x_2, x_3, ..., x_r)$, $\mathbf{x} \in \Re^r$. If $f(\mathbf{x})$ turns out to be positive, it belongs to the novice class; otherwise, it belongs to the expert class. The input vector $\mathbf{x}$ is projected down to one dimension using $\mathbf{y} = f(\mathbf{x}) = (\mathbf{w})^T\mathbf{x} + b$ where $\mathbf{w} \in \Re^r$ is the weight vector. Alternatively, the formula can be rewritten in matrix form:

$$
\begin{aligned}
y &= \mathbf{X} \quad . \quad \mathbf{c} \\
where \quad \mathbf{X} &= \begin{pmatrix} \mathbf{x} \\ \\ 1 \end{pmatrix}^T \quad and \\
c &= \begin{pmatrix} \mathbf{w} \\ \\ b \end{pmatrix}
\end{aligned}
\tag{4.1}
$$

Both the weight vector $\mathbf{w}$ and b can be found by using the FLD method or the SVM method.

4.4.1 Fisher Linear Discriminant(FLD)

The FLD approach first finds the weights of the hyperplane on which the projection of the data is maximally distinguished (Bishop and Nasrabadi, 2006). The elements of the weight vector $\mathbf{f}_w$ are found by using Equations 4.2. Let J be the set of indexes representing the novice training samples and S correspondingly be the set representing the expert training samples. NJ defines as the total number of sample points in the novice group and the NS defines as the total number of sample points in the expert group. The input vector $\mathbf{x}$ refers to each input feature vector whose elements are selected by using the feature selection methods explained in the previous session.

$$\begin{aligned} f_{(w)} &= \frac{(\mu_J - \mu_S)^2}{\sigma_J^2 + \sigma_S^2} \\ \mu_J &= \frac{1}{\mathrm{NJ}} \sum_{i \in J} x_i \\ \mu_S &= \frac{1}{\mathrm{NS}} \sum_{i \in S} x_i \\ \sigma_J &= \sum_{i \in J} (x_i - \mu_J)^2 \quad \sigma_S = \sum_{i \in S} (x_i - \mu_S)^2 \end{aligned} \tag{4.2}$$

Then, the coefficients of the hyperplane between the skill performance of surgeons are defined by using the regression Equations 4.3: $\mathbf{x}$=$\mathbf{A}_r \cdot \mathbf{f}_w$, where $\mathbf{A}_r \in \Re^{m \times r}$ and $\mathbf{f}_w \in \Re^r$, a label vector $\mathbf{t} \in \Re^m$ includes +1 which represents the skill performance of a novice surgeon and -1 which represents the skill performance of an expert surgeon.

$$\begin{aligned} &\underset{c}{\text{minimize}} \quad ||\mathbf{Xc} - \mathbf{t}||_2^2 \\ &\mathbf{t} = [+1 \cdots -1]^T \\ &\mathbf{X} \text{ and } \mathbf{c} \text{ are as defined in formula 4.1} \end{aligned} \tag{4.3}$$

Thus, the skill performance of each surgeon is predicted by first multiplying the four selected features with the weight vector $\mathbf{f}_w$. Then, the outcome is determined by using Formula 4.1 with $\mathbf{w}$ and b found in Equation 4.3.

4.4.2 Support Vector Machine(SVM)

The SVM classifier finds an optimal hyperplane that maximizes the margin between data points in two different classes (Statnikov *et al.*, 2011). The weight vector **w** and b can be found by the following equation:

$$\begin{aligned} \underset{w,b,\xi}{\text{minimize}} \quad & \frac{1}{2}||\mathbf{w}||_2^2 + C\sum_{j=1}^{N}\xi_j \\ \text{subject to} \quad & y_i((\mathbf{w}.\mathbf{x}_i) + b \geq 1 - \xi_i \; for \; i = 1, \ldots, N. \\ & \xi_i \geq 0 \end{aligned}$$

where there are N samples $(x_1, x_2..., x_N)$ and corresponding classification labels $(y_1, y_2..., y_N \in \{-1, +1\})$. Under the constraint $y_i((\mathbf{w}.\mathbf{x}_i) + b \geq 1 - \xi_i$, the error is bounded by slack variables ξ_i. $C \geq 0$ is a user-defined parameter. In this above method, the computation cost for finding the weight vector is high. Alternatively, it can be reformulated into dual form to reduce the computational cost. The equation is as follows: $\boldsymbol{\alpha} = (\alpha_1, \alpha_2, \alpha_3, ..., \alpha_N)$

$$\begin{aligned} \underset{\alpha}{\text{minimize}} \quad & \frac{1}{2}\sum_{j,k=1}^{N}\alpha_j\alpha_k y_j y_k \mathbf{x}_j.\mathbf{x}_k - \sum_{j=1}^{N}\alpha_j \\ \text{subject to} \quad & \sum_{i=1}^{N}\alpha_i y_i = 0 \; for \; i = 1, \ldots, N. \\ & 0 \leq \alpha_i \leq C \end{aligned}$$

$$\mathbf{w} = \sum_{j=1}^{N}\alpha_j y_j \mathbf{x}_j \tag{4.4}$$

$$b = -\frac{1}{2}(\mathbf{w}.\mathbf{x}_i \; + \; \mathbf{w}.\mathbf{x}_j) = -\frac{1}{2}\sum_{k=1}^{N}\alpha_k y_k(\mathbf{x}_k.\mathbf{x}_j + \mathbf{x}_k.\mathbf{x}_i) \tag{4.5}$$

where $\mathbf{x}_i$ and $\mathbf{x}_j$ are two arbitrary objects with different classification labels and $0 \leq \alpha_i \leq C$ and $0 \leq \alpha_j \leq C$. $C \geq 0$ is a user-defined parameter. If C is set to be large, each non-zero ξ_i has a large contribution; thus, the margin is big. If C is set to be small, each non-zero ξ_i has a small contribution; thus, the margin is small and there is a higher chance of being misclassified. C is adjusted by using the result from the evaluation as discussed in the next section. The svmtrain function in MATLAB®'s Statistics Toolbox is used to classify the skill performance by an expert

or a novice.

According to Formula 4.1, the skill performance of each surgeon is predicted by multiplying the selected features **x** with the weight vector from Formula 4.4 and the constant given from Formula 4.5.

4.5 Evaluation

Two techniques that validate this machine learning approach are hold-out cross-validation and leave-n-out cross validation methods (Statnikov *et al.*, 2011). The hold-out cross-validation method requires to split the data set into a training set and a testing set. The classifier is built using the training set of data and the evaluation on the machine learning approach is determined by using the testing set. Although hold-out cross validation is the most practical approach to evaluate the machine learning, it requires a large sample size.

In the leave-one-out cross validation method, the classifier is built on all data except for the one sample that is left out for testing. The leave-one-out classifier is evaluated on the removed sample to determine whether it predicts correctly. These steps are repeated for every test sample so that there are N tests in total. The final accuracy is the average of correct predictions. In this way, the leave-one-out method tests all the available data.

Because there are eight subjects for each group, the sample size is too small to use the hold-out cross validation method. Instead, the leave-one-out cross validation method is used to evaluate the machine learning approach. The parameter C, which is required to adjust the SVM, is determined by achieving the highest correct percentage prediction upon evaluation.

4.6 Results

The results of the surgeons' skill performance for the peg transfer task are listed in Tables 4.6 – 4.9. They are summarised as follows:

1. PCA feature selection with FLD classifier predicts 69% correctly.
2. PCA feature selection with SVM classifier predicts 68% correctly.
3. mRMR feature selection with FLD classifier predicts 73% correctly.
4. mRMR feature selction with SVM classifer predicts 69% correctly.

Table 4.6: Evaluation Results from using the PCA Feature Selection with the FLD Classifier

Group	# of correct predictions	# of wrong predictions	percent correct
Expert	18	6	75
Novice	15	9	63
Total	33	15	69

Table 4.7: Evaluation Results from using the PCA Feature Selection with the SVM Classifier

Group	# of correct predictions	# of wrong predictions	percent correct
Expert	18	6	75
Novice	14	10	58
Total	32	16	67

Table 4.8: Evaluation Results from using the mRMR Feature Selection with the FLD Classifier

Group	# of correct predictions	# of wrong predictions	percent correct
Expert	18	6	75
Novice	17	7	71
Total	35	13	73

Table 4.9: Evaluation Results from using the mRMR Feature Selection with the SVM Classifier

Group	# of correct predictions	# of wrong predictions	percent correct
Expert	16	8	67
Novice	17	7	71
Total	33	15	69

4.7 Metric Scales using the Results from the Machine Learning Method

Similar to the statistical method as discussed in Chapter 3, the most relevant feature in each category is extracted by using the mutual information, minimum redundancy and maximum feature selection method. The most relevant features in each category are

1. total time taken
2. total length moved by the surgeon's right hand along the x-axis
3. average speed of the surgeon's right hand using the norm formula while picking five pegs from the surgeon's right to the left side
4. smoothness of movement of the surgeon's right hand using the norm formula while picking all five pegs from the surgeon's right to the left side
5. total number of up and down movements by the surgeon's right hand

The metric scales to measure the performance of the peg transfer task are achieved by applying Algorithm 1 as mentioned in Chapter 3. Figure 4.17 shows the scores that are achieved by all surgeons while performing three trials of the peg transfer task. The scores were better for more experienced surgeons.

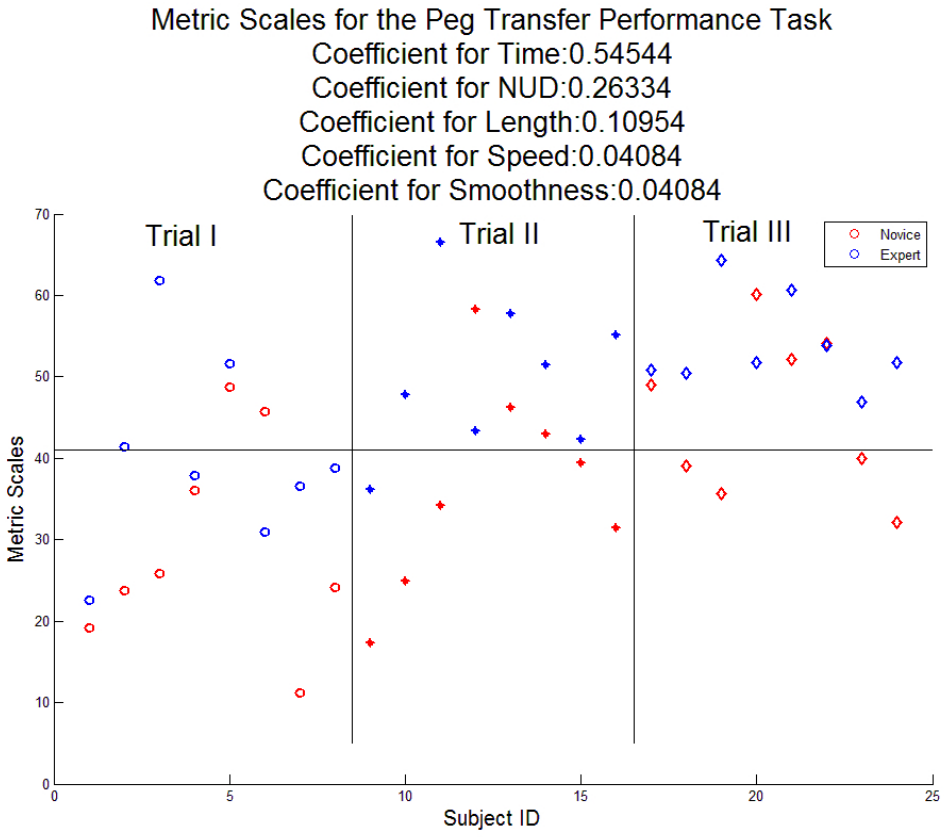

Figure 4.17: Metric Scales for the Peg Transfer Task

Chapter 5

Ergonomic Analysis:Wrist Posture

In this chapter, the wrist angle trajectories are utilized to analyse the ergonomic performance of a surgeon using the same methods and steps described in Chapter 3 and Chapter 4 (Figure 5.1). The goal is to provide feedback to a surgeon on the task execution ergonomics.

As mentioned in the data acquisition section, while manipulating the grasper handles for both tasks, the surgeons' wrist postures are exposed to extension, flexion, radial deviation and ulnar deviation. The wrist angles are measured using two EMI sensors: one mounted on the forearm and another one mounted on the back of the hand. The sensors' axes are parallel when the hand is at the steady posture. Wrist extension results in a positive angle difference between two sensors along the y-axis, whereas wrist flexion results in a negative angle difference between two sensors along the y-axis. Wrist ulnar deviation results in a positive angle difference between two sensors along the z-axis, whereas wrist radial deviation results in a negative angle difference between two sensors along the z-axis. Wrist extension, flexion, radial deviation and ulnar deviation are grouped into three categories: neutral posture, moderate stress and severe stress.

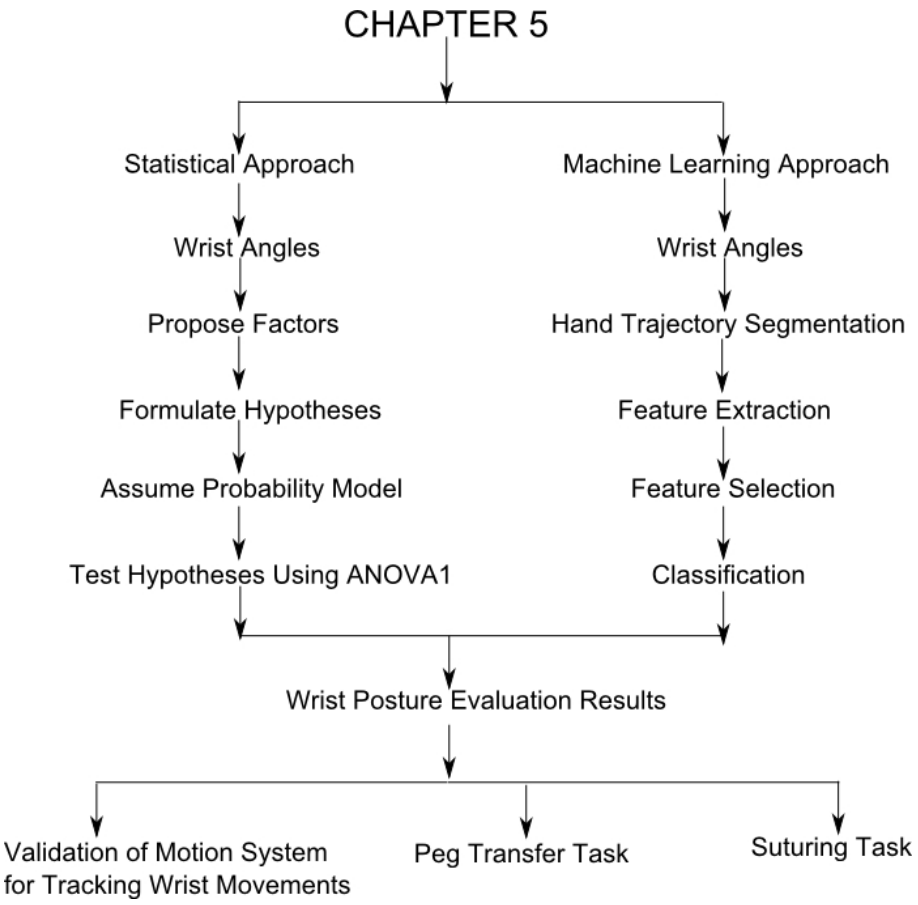

Figure 5.1: Chapter 5 Outline

In each category, factors that may contribute to the ergonomic performance of the surgeons' wrist angles are proposed by using Formula 5.1. Using these factors, hypotheses are formulated to determine whether the ergonomic performance between novice and expert surgeons is distinguishable. The same probability model and steps described in Chapter 3 are applied to test hypotheses. The factors, which are rejected by the hypotheses, are proved to statistically distinguish the ergonomic performance between novice and expert surgeons. Because the factors discriminate the ergonomic performance between novice and expert surgeons, the Ascension 3DGuidance trakSTAR system for tracking wrist movements is validated. The average wrist stress levels of surgeons while performing both tasks are also reported.

The machine learning method, as discussed in Chapter 4, predicts the ergonomic performance of a surgeon. Wrist angle segmentation is achieved by grouping all the positive or negative angle differences along the y-axis and grouping all the positive or negative angle differences along the z-axis. Features are extracted using the same Formula 5.1 as in the statistical method. Applying the same four models as discussed in Chapter 4 leads to the prediction of the ergonomic performance of a surgeon: PCA feature selection with FLD classifier, PCA feature selection with SVM classifier, mRMR feature selection with FLD classifier, and mRMR feature selection with SVM classifier. The leave-one-out cross validation method is also used to evaluate this machine learning algorithm.

$$\%t = \frac{100}{T} \cdot \sum_{i=1}^{k} t_i \tag{5.1}$$

T is defined as total time taken and t_i is defined as the duration under each category in each group. %t is defined as the percent time spent under each category in each group.

5.1 Statistical Method

Factors that may contribute to surgeons' ergonomic performance on wrist angles are listed in Table 5.1. Factors are defined through experimenting the degree of differentiating the ergonomic performance between novice and expert surgeons. Consequently, the degree range for each category may just apply to this acquired data.

Table 5.1: Wrist posture Analysis Factor

Factor	Category	Side	Angle Range	Formula
Extension	Neutral	L.H.	$0\,^{\circ} \leq \Theta_{\mathrm{EXT}} < 16^{\circ}$	$\%t = \frac{100}{T} \cdot \sum_{i=1}^{k} t_i$
		R.H.	$0\,^{\circ} \leq \Theta_{\mathrm{EXT}} < 16^{\circ}$	
	Moderate	L.H.	$16\,^{\circ} \leq \Theta_{\mathrm{EXT}} < 46^{\circ}$	
		R.H.	$16\,^{\circ} \leq \Theta_{\mathrm{EXT}} < 46^{\circ}$	
	Severe	L.H.	$46\,^{\circ} \leq \Theta_{\mathrm{EXT}} < 90^{\circ}$	
		R.H.	$46\,^{\circ} \leq \Theta_{\mathrm{EXT}} < 90^{\circ}$	
Flexion	Neutral	L.H.	$-16\,^{\circ} \leq \Theta_{\mathrm{FLEX}} < 0^{\circ}$	$\%t = \frac{100}{T} \cdot \sum_{i=1}^{k} t_i$
		R.H.	$-16\,^{\circ} \leq \Theta_{\mathrm{FLEX}} < 0^{\circ}$	
	Moderate	L.H.	$-46\,^{\circ} \leq \Theta_{\mathrm{FLEX}} < -16^{\circ}$	
		R.H.	$-46\,^{\circ} \leq \Theta_{\mathrm{FLEX}} < -16^{\circ}$	
	Severe	L.H.	$-90\,^{\circ} \leq \Theta_{\mathrm{FLEX}} < -46^{\circ}$	
		R.H.	$-90\,^{\circ} \leq \Theta_{\mathrm{FLEX}} < -46^{\circ}$	
Ulnar Deviation	Neutral	L.H.	$0^{\circ} \leq \Psi_{\mathrm{RAD}} < 10^{\circ}$	$\%t = \frac{100}{T} \cdot \sum_{i=1}^{k} t_i$
		R.H.	$0^{\circ} \leq \Psi_{\mathrm{RAD}} < 10^{\circ}$	
	Moderate	L.H.	$10^{\circ} \leq \Psi_{\mathrm{RAD}} < 60^{\circ}$	
		R.H.	$10^{\circ} \leq \Psi_{\mathrm{RAD}} < 60^{\circ}$	
	Severe	L.H.	$60^{\circ} \leq \Psi_{\mathrm{RAD}} < 90^{\circ}$	
		R.H.	$60^{\circ} \leq \Psi_{\mathrm{RAD}} < 90^{\circ}$	
Radial Deviation	Neutral	L.H.	$-15^{\circ} \leq \Psi_{\mathrm{ULN}} < 0^{\circ}$	$\%t = \frac{100}{T} \cdot \sum_{i=1}^{k} t_i$
		R.H.	$-15^{\circ} \leq \Psi_{\mathrm{ULN}} < 0^{\circ}$	
	Moderate	L.H.	$-60^{\circ} \leq \Psi_{\mathrm{ULN}} < -15^{\circ}$	
		R.H.	$-60^{\circ} \leq \Psi_{\mathrm{ULN}} < -15^{\circ}$	
	Severe	L.H.	$-90^{\circ} \leq \Psi_{\mathrm{ULN}} < -60^{\circ}$	
		R.H.	$-90^{\circ} \leq \Psi_{\mathrm{ULN}} < -60^{\circ}$	

Using the defined factors, the following hypotheses are formulated for both the peg transfer task and suturing task:

1. The means of the extension factors are the same.
2. The means of the flexion factors are the same.
3. The means of the radial deviation factors are the same.
4. The means of the ulnar deviation factors are the same.

5.1.1 Results

The following results are obtained using the same assumption of the probability model and ANOVA1 function as discussed in Chapter 3. As depicted in the following figures, the null hypotheses for the respective factors can be rejected because the corresponding p-values are all less than 0.05. Therefore, these factors are proved to statistically distinguish the ergonomic performance between novice and expert surgeons. Consequently the Ascension 3DGuidance trakSTAR system for tracking wrist movements is validated.

Peg Transfer Results

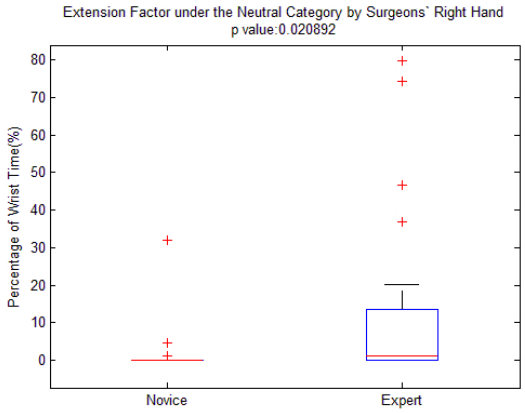

Figure 5.2: Time range of wrist extension under the neutral category by novices' right hand is from 0% to 29% whereas the time range of wrist extension by experts' right hand is from 0% to 73%.

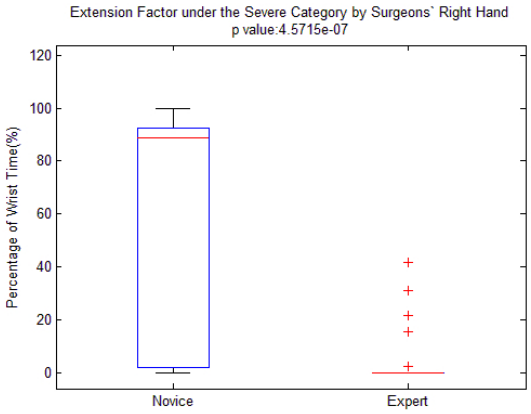

Figure 5.3: Time range of wrist extension under the severe category by novices' right hand is from 0% to 99% whereas the time range of wrist extension by experts' right hand is from 0% to 43%.

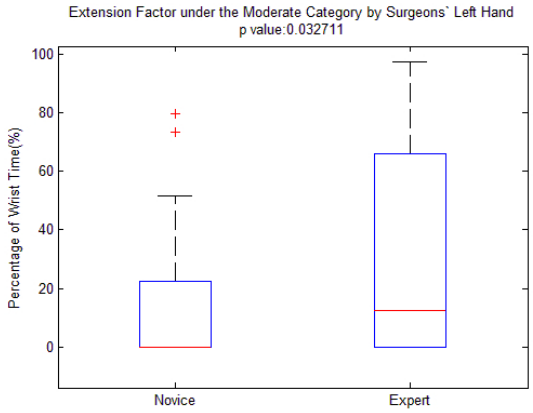

Figure 5.4: Time range of wrist extension under the moderate category by novices' left hand is from 0% to 79% whereas the time range of wrist extension by experts' left hand is from 0% to 97%.

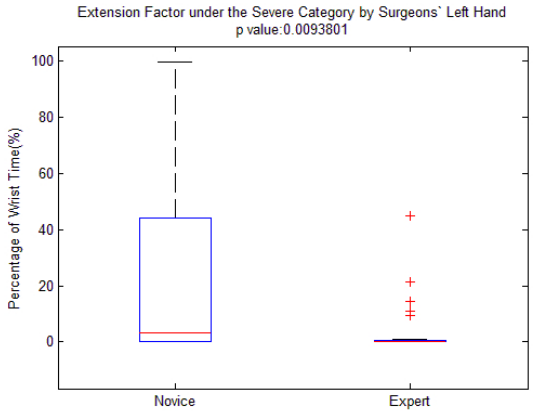

Figure 5.5: Time range of wrist extension under the severe category by novices' left hand is from 0% to 100% whereas the time range of wrist extension by experts' left hand is from 0% to 45%.

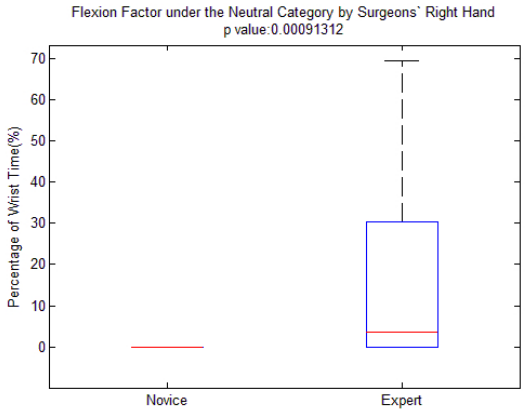

Figure 5.6: No novices are found with wrist flexion under the neutral category by the right hand, whereas the time range of wrist flexion by experts' right hand is from 0% to 68%.

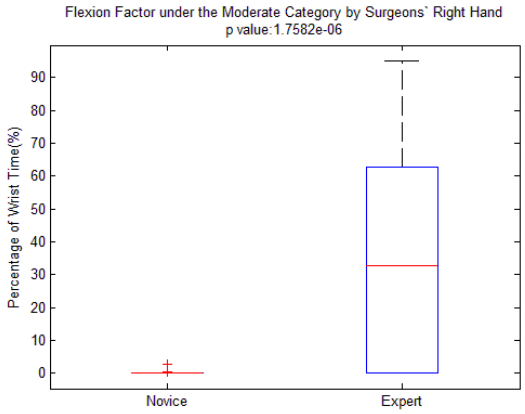

Figure 5.7: Time range of wrist flexion under the moderate category by novices' right hand is from 0% to 1.7% whereas the time range of wrist flexion by experts' right hand is from 0% to 95%.

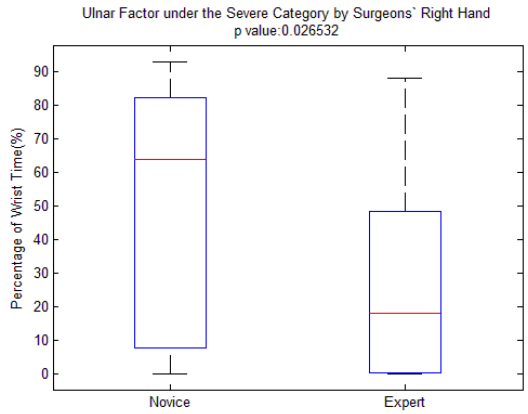

Figure 5.8: Time range of wrist ulnar deviation under the severe category by novices' right hand is from 0% to 93% whereas the time range of wrist ulnar deviation by experts' right hand is from 0% to 88%.

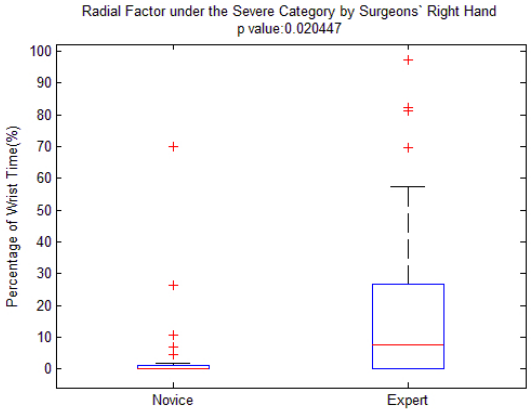

Figure 5.9: Time range of wrist radial deviation under the severe category by novices' right hand is from 0% to 70% whereas the range of wrist radial deviation by experts' right hand is from 0% to 97%.

Suturing Task Results

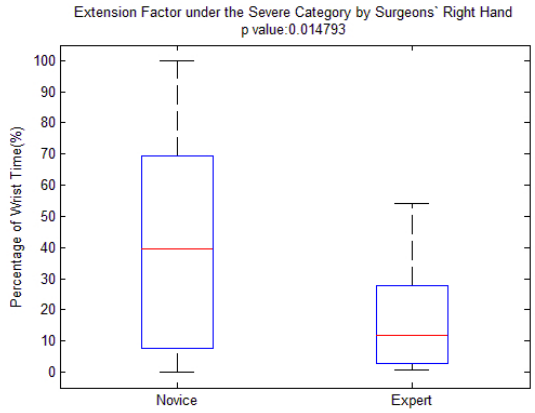

Figure 5.10: Time range of wrist extension under the severe category by novices' right hand is from 0% to 99% whereas the time range of wrist extension by experts' right hand is from 0.6% to 54%.

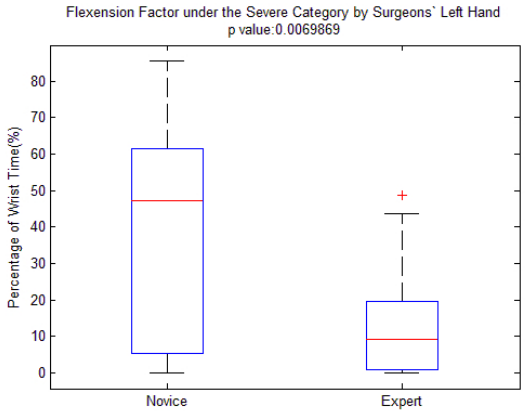

Figure 5.11: Time range of wrist flexion under the severe category by novices' left hand is from 0% to 87% whereas the time range of wrist flexion by experts' left hand is from 0% to 49%.

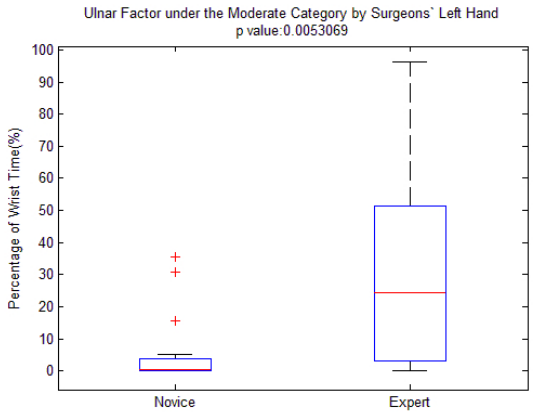

Figure 5.12: Time range of wrist ulnar deviation under the moderate category by novices' left hand is from 0% to 35% whereas the time range of wrist ulnar deviation by experts' left hand is from 0% to 96%.

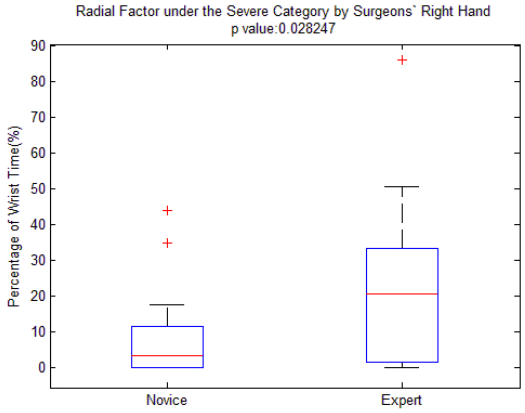

Figure 5.13: Time range of wrist radial deviation under the severe category by novices' right hand is from 0% to 43% whereas the time range of wrist radial deviation by experts' right hand is from 0% to 89%.

Posture Analysis for Peg Transfer Task

Table 5.2 indicates the average wrist stress levels of surgeons while performing the peg transfer task. The notations N.L., M.L. and S.L. are defined as neutral, moderate and severe wrist stress levels respectively. L.H. refers to a surgeon's left hand whereas R.H. refers to a surgeon's right hand. All surgeons could be analytically aware of the ergonomic problem by making the stress levels on surgeons' wrist postures available during the training. This awareness may lead a surgeon to perform the task in an ergonomic manner. Thus, the average wrist stress levels of surgeons while performing peg transfer task is reported.

Table 5.2: Mean Percentage of wrist time spent in a position and stress level

		Stress Level					
		N.L. by L.H.	M.L. by L.H.	S.L. by L.H.	N.L. by R.H.	M.L. by R.H.	S.L.by R.H.
Extension	Novice	11%	14%	24%	2%	11%	58%
	Expert	11%	34%	4%	13%	11%	5%
Flexion	Novice	11%	16%	18%	0%	0%	23%
	Expert	4%	33%	9%	15%	36%	14%
Ulnar	Novice	4%	14%	25%	4%	33%	50%
	Expert	1%	21%	16%	1%	35%	28%
Radial	Novice	4%	20%	27%	1%	0 %	5%
	Expert	3%	39%	14%	1%	8%	22%

Posture Analysis for Suturing Task

Table 5.3 indicates the average wrist stress levels of surgeons while performing the suturing task.

Table 5.3: Mean Percentage of wrist time spent in a position and stress level

		Stress Level					
		N.L. by L.H.	M.L. by L.H.	S.L. by L.H.	N.L. by R.H.	M.L. by R.H.	S.L.by R.H.
Extension	Novice	9%	11%	16%	7%	22%	42%
	Expert	19%	11%	21%	7%	13%	18%
Flexion	Novice	10%	15%	39%	3%	8%	16%
	Expert	15%	19%	14%	11%	21%	29%
Ulnar	Novice	3%	6%	9%	5%	24%	10%
	Expert	5%	32%	18%	2%	23%	22%
Radial	Novice	11%	44%	27%	10%	42 %	9%
	Expert	5%	26%	15%	5%	24%	24%

5.2 Machine Learning Method

5.2.1 Hand Trajectory Segmentation

The segmentation for wrist extension is obtained by grouping all the positive angle differences along the y-axis, whereas segmentation for wrist flexion is obtained by grouping all the negative angle differences along the y-axis. The segmentation for wrist ulnar deviation is obtained by grouping all the positive angle differences along the z-axis, whereas segmentation for wrist radial deviation is obtained by grouping all the negative angle differences along the z-axis.

5.2.2 Feature Extraction

Similar to the statistical method, there are six features related to the extension, six features related to the flexion, six features related to the radial deviation, and six features related to the ulnar deviation. The features, which are extracted by using the same Formula 5.1, are defined as in Table 5.1.

5.2.3 Peg Transfer Task Results by Feature Selection

Principal Component Analysis(PCA)

Using the PCA method discussed in Chapter 4, eigenvector features that have the six largest eigenvalues are assumed to represent surgeons' ergonomic performance on wrist angles for the peg transfer task. The exact number is left as future research, when there are more data available to analyse.

Minimum Redundancy and Maximum Relevance Feature Selection (mRMR)

Using the mRMR method discussed in Chapter 4, the following five best features are assumed to represent surgeons' ergonomic performance on wrist angles during the peg transfer task execution:

1. Extension feature under the severe category by surgeon's right hand
2. Radial feature under the neutral category by surgeon's left hand
3. Ulnar feature under the moderate category by surgeon's right hand
4. Flexion feature under the moderate category by surgeon's right hand
5. Extension feature under the neutral category by surgeon's right hand

5.2.4 Peg Transfer Task Results by Classification and Evaluation

Using the same FLD classifier, SVM classifier and evaluation method, the evaluation results of surgeons' ergonomic performance on wrist angles during the peg transfer task execution are listed in Tables 5.4 – 5.7. They are summarised as follows:

1. PCA feature selection with FLD classifier predicts 88% correctly.
2. PCA feature selection with SVM classifier predicts 88% correctly.
3. mRMR feature selection with FLD classifier predicts 60% correctly.
4. mRMR feature selection with SVM classifier predicts 75% correctly.

Table 5.4: Evaluation Results from using the PCA Feature Selection with the FLD Classifier

Group	# of correct predictions	# of wrong predictions	percent correct
Expert	20	4	83
Novice	22	2	92
Total	42	6	88

Table 5.5: Evaluation Results from using the PCA Feature Selection with the SVM Classifier

Group	# of correct predictions	# of wrong predictions	percent correct
Expert	20	4	83
Novice	22	2	92
Total	42	6	88

Table 5.6: Evaluation Results from using the mRMR Feature Selection with the FLD Classifier

Group	# of correct predictions	# of wrong predictions	percent correct
Expert	14	10	58
Novice	15	9	63
Total	29	19	60

Table 5.7: Evaluation Results from using the mRMR Feature Selection with the SVM Classifier

Group	# of correct predictions	# of wrong predictions	percent correct
Expert	20	4	83
Novice	16	8	67
Total	36	12	75

5.2.5 Suturing Task Results by Feature Selection

Using the PCA method discussed in Chapter 4, eigenvector features that have four large eigenvalues are assumed to represent surgeons' ergonomic performance on wrist angles during the suturing task execution. The exact number is left as future research when there are more data available to analyse.

Minimum Redundancy and Maximum Relevance Feature Selection (mRMR)

Using the mRMR method discussed in Chapter 4, the following three best features are assumed to represent surgeons' ergonomic performance on wrist angles during the suturing task execution:

1. Radial feature under the neutral category by surgeon's left hand
2. Radial feature under the neutral category by surgeon's right hand
3. Ulnar feature under the moderate category by surgeon's left hand

5.2.6 Suturing Task Results by Classification and Evaluation

Using the same FLD classifier, SVM classifier and evaluation method, the evaluation results of the ergonomic performance on surgeons' wrist angles during the suturing task execution are listed in Tables 5.8 – 5.11. They are summarised as follows:

1. PCA feature selection with FLD classifier predicts 75% correctly.
2. PCA feature selection with SVM classifier predicts 75% correctly.
3. mRMR feature selection with FLD classifier predicts 59% correctly.
4. mRMR feature selection with SVM classifier predicts 66% correctly.

Table 5.8: Evaluation Results from using the PCA Features Selection with the FLD Classifier

Group	# of correct predictions	# of wrong predictions	percent correct
Expert	13	3	81
Novice	12	4	75
Total	25	7	75

Table 5.9: Evaluation Results from using the PCA Features Selection with the SVM Classifier

Group	# of correct predictions	# of wrong predictions	percent correct
Expert	12	4	75
Novice	12	4	75
Total	24	8	75

Table 5.10: Evaluation Results from using the mRMR Feature Selection with the FLD Classifier

Group	# of correct predictions	# of wrong predictions	percent correct
Expert	11	5	69
Novice	8	8	50
Total	19	13	59

Table 5.11: Evaluation Results from using the mRMR Feature Selection with the SVM Classifier

Group	# of correct predictions	# of wrong predictions	percent correct
Expert	11	5	69
Novice	10	6	63
Total	21	11	66

Chapter 6

Conclusions and Discussion

Training and ergonomics evaluation for laparoscopic surgery aim to help a surgeon improve hand dexterity, evaluate hand movement precision and perform surgery in an ergonomic manner. This type of evaluation is developed through a system that captures the positions and orientations of hand and laparoscopic tool movements, records these acquired data, and converts these recorded data into a feedback training evaluation tool. While the Ascension 3DGuidance trakSTAR tracking system acquires the positions and orientations of hand and laparoscopic tool movements, both statistical and machine learning methods convert the captured data into a feedback training evaluation tool. The data acquisition technique includes developing software to record data and then converting the recorded data into skill and wrist ergonomic analysis data. The statistical approach covers the topics of defining the measurement variables, proposing hypotheses, assuming probability models and testing hypotheses. The machine learning approach lists out the steps and methods: hand trajectory segmentation, feature extraction, feature selection, classification and evaluation. Thus, the outcome of the proposed evaluation system is quantitative, automatic and objective.

Seven PGY1 laparoscopic residents, one general surgery resident, and eight PGY4 residents and urology fellows performed three trials of the peg transfer task and two trials of the suturing task. The Ascension 3DGuidance trakSTAR tracker was used to capture the positions and orientations of the EMI sensors, which were mounted on surgeons' hands, forearms and elbows. The sensors were

also fitted onto the handle of laparoscopic tools. The acquired data were recorded by custom software. The recorded laparoscopic handle trajectory was then converted into tip trajectory through estimating the tip positions referenced to the handle positions by either the eigenvalue decomposition method or the pivot-calibration method. The eigenvalue decomposition method resulted in higher accuracy than the pivot-calibration method for this tracking system. The hand and forearm trajectories were transformed into wrist angle trajectories. Both statistical and machine learning methods transformed the tip trajectory into metrics that were used to evaluate the skill performance of a surgeon. Both methods also transformed the wrist angle trajectory into metrics that were used to evaluate the ergonomic performance of a surgeon.

Under the statistical approach, factors are proved to differentiate technical skills between novice and expert surgeons for the peg transfer task. Consequently, the proposed motion measurement system is validated for tracking laparoscopic tip movements. Under each category of factors, the factor with the highest confidence level of differentiating the skill performance between surgeons is extracted. Using these factors, the algorithm to determine the metric scale for each surgeon's performance is proposed. This proposed competency-based score system is intended to help novices learn faster by achieving greater economy and higher efficiency.

Under the machine learning approach, hand movement evaluation is proposed by first automatically segmenting hand trajectory. The segmentation is also intended to provid feedback on surgical performance in a quantitative, automatic and objective manner. With the aid of segmentation, features are proposed to predict the skill performance of a surgeon. Features that are most statistically dependence on the skill performance between novice and expert surgeons are selected to avoid the dimensionality problem. Specifically, four models that select features and predict the skill performance of a surgeon are proposed: PCA feature selection with FLD classifier, PCA feature selection with SVM classifier, mRMR feature selection with FLD classifier, and mRMR feature selection with SVM classifier. These four models are validated by the leave-one-out cross validation method. mRMR feature selection with FLD classifier models gives the highest percentage of correct classification which is 73%. The alternative approach of developing the competency-based score system is obtained by using mRMR feature selection with the mentioned metric scale algorithm.

Using the same methods that are applied for the skill evaluation, the ergonomic analysis on

wrist angles is proposed. The statistical approach proves that the proposed factors distinguish the ergonomic performance on surgeons' wrist angles for both tasks. Both PCA feature selection with SVM classifier and PCA feature selection with SVM classifier give the highest percentage of correct classification for both tasks: 88% for the peg transfer and 75% for the suturing task.

All surgeons could be analytically aware of the ergonomic problem by making the stress levels on surgeons' wrist postures available during the training. This awareness may lead a surgeon to perform the task in an ergonomic manner. Thus, the average wrist stress levels of surgeons while performing both tasks are also reported. The ergonomic analysis may help an engineer design a new handle so that a surgeon could avoid severe and moderate stress levels of wrist posture. Alternatively, the analysis and segmentation may help a researcher find ergonomic and efficient ways to perform surgical tasks. Although more data are still required to make a general claim about the results, the proposed system and methods are designed to be used as tools for further research in training and ergonomics evaluation for laparoscopic surgery.

6.1 Discussion

The analysis on the skill and wrist angles of eight subjects in either a novice or expert group does not include enough data to draw a general conclusion. However, the proposed system and approaches are designed to be treated as preliminary research on acquiring and analysing motion data. Although the Ascension 3DGuidance trakSTAR has the ability to track the positions and orientations of an object in 3D space, inconsistent offset errors in capturing data are randomly recorded. These errors have led to the inability to track surgeons' performance precision. As a result of these errors, the proposed algorithm to segment the path of picking, transferring and placing a peg contains more steps than required.

If the threshold value between low- and high frequencies for the smoothness factor is obtained through an optimization method, the results may lead to better accuracy compared with experimentally examining the degree of differentiating the skill performance between novice and expert surgeons. The projection of the data on the lower dimensional linear space is not always the best for selecting features because larger eigenvalues may make two groups coincide whereas the smaller eigenvalues may separate the two groups (Theodoridis, 2003). The mRMR is based on greedy

methods that select individual features one at a time. Thus, it may discard sets of features which individually are not discriminative, but jointly are highly discriminative (Khodayari-Rostamabad *et al.*, 2013). In order to validate the competency-based score method, the data measurements with known different technical skill levels of surgeons are required. Hold-out cross validation is a more practical approach to evaluate the machine learning; more data are still required.

6.2 Further Development

Further development could include: –

- Finding a way to remove inconsistent offset errors in data acquisition so that the skill performance precision can be tracked.
- Validating recorded wrist angles data while performing the surgical tasks so that ergonomic analysis fulfils its intended purpose
- Validating wrist stress levels using the Ascension 3DGuidance trakSTAR system so that ergonomic analysis fulfils its intended purpose
- Obtaining more data so that a general conclusion can be drawn
- Finding actual hand tremor frequency using the Ascension 3DGuidance trakSTAR system to fulfil its intended purpose.
- Research on other feature selection methods so that the skill evaluation fulfils its intended purpose
- Finding the exact number of features required to represent samples through an optimization method so that the skill evaluation fulfils its intended purpose
- Validating the competency-based score method by acquiring data measurements with known different technical skill levels of surgeons to fulfil its intended purpose
- Analysing wrist supination and pronation for ergonomic analysis

Bibliography

Alpaydin, E. (2010). *Introduction to Machine Learning*. The MIT Press.

Atug, F., Castle, E. P., Woods, M., Davis, R., and Thomas, R. (2006). Robotics in urologic surgery: an evolving new technology. *International journal of urology*, **13**(7), 857–863.

Barnes, R. M. and Barnes, R. M. (1958). *Motion and time study*, volume 84. Wiley.

Berguer, R., Forkey, D., and Smith, W. (1999). Ergonomic problems associated with laparoscopic surgery. *Surgical Endoscopy*, **13**(5), 466–468.

Bishop, C. M. and Nasrabadi, N. M. (2006). *Pattern Recognition and Machine Learning*. Springer.

Chambers, J. M. (1983). *Graphical methods for data analysis*.

Darzi, A., Smith, S., and Taffinder, N. (1999). Assessing operative skill: needs to become more objective. *BMJ: British Medical Journal*, page 318:887.

Datta, V., Mackay, S., Mandalia, M., and Darzi, A. (2001). The use of electromagnetic motion tracking analysis to objectively measure open surgical skill in the laboratory-based model. *Journal of the American College of Surgeons*, **193**(5), 479–485.

Datta, V., Chang, A., Mackay, S., and Darzi, A. (2002). The relationship between motion analysis and surgical technical assessments. *The American Journal of Surgery*, **184**, 70–73.

Derossis, A., Bothwell, J., Sigman, H., and Fried, G. (1998). The effect of practice on performance in a laparoscopic simulator. *Surgical endoscopy*, **12**(9), 1117–1120.

Derossis MD, A. M., Fried MD, G. M., Abrahamowicz PhD, M., Sigman MD, H. H., Barkun MD, J. S., and Meakins MD, J. L. (1998). Development of a model for training and evaluation of laparoscopic skills. *The American journal of surgery*, **175**(6), 482–487.

Devore, J. (2012). *Probability & Statistics for Engineering and the Sciences*. CengageBrain. com.

Ding, C. and Peng, H. (2005). Minimum redundancy feature selection from microarray gene expression data. *Journal of bioinformatics and computational biology*, **3**(02), 185–205.

Dosis, A., Aggarwal, R., Bello, F., Moorthy, K., Munz, Y., Gillies, D., and Darzi, A. (2005). Synchronized video and motion analysis for the assessment of procedures in the operating theater. *Archives of Surgery*, **140**(3), 293.

Egi, H., Okajima, M., Yoshimitsu, M., Ikeda, S., Miyata, Y., Masugami, H., Kawahara, T., Kurita, Y., Kaneko, M., and Asahara, T. (2008). Objective assessment of endoscopic surgical skills by analyzing direction-dependent dexterity using the hiroshima university endoscopic surgical assessment device (huesad). *Surgery today*, **38**(8), 705–710.

Falcone, J. L., Chen, X., and Hamad, G. G. (2012). The traveling salesman problem in surgery: economy of motion for the fls peg transfer task. *Surgical endoscopy*, pages 1–6.

Faria, D. R. and Dias, J. (2009). 3d hand trajectory segmentation by curvatures and hand orientation for classification through a probabilistic approach. In *Intelligent Robots and Systems, 2009. IROS 2009. IEEE/RSJ International Conference on*, pages 1284–1289. IEEE.

Flanagan, J. R., Bowman, M. C., and Johansson, R. S. (2006). Control strategies in object manipulation tasks. *Current opinion in neurobiology*, **16**(6), 650–659.

Grant, M. and Boyd, S. (2013). CVX: Matlab software for disciplined convex programming, version 2.0 beta.

Hatzinger, M., Kwon, S., Langbein, S., Kamp, S., Häcker, A., and Alken, P. (2006). Hans christian jacobaeus: Inventor of human laparoscopy and thoracoscopy. *Journal of endourology*, **20**(11), 848–850.

Hemal, A., Srinivas, M., and Charles, A. (2001). Ergonomic problems associated with laparoscopy. *Journal of endourology*, **15**(5), 499–503.

Johansson, R. S. and Cole, K. J. (1992). Sensory-motor coordination during grasping and manipulative actions. *Current opinion in neurobiology*, **2**(6), 815–823.

Khodayari-Rostamabad, A., Reilly, J. P., Hasey, G. M., de Bruin, H., and MacCrimmon, D. J. (2013). A machine learning approach using eeg data to predict response to ssri treatment for major depressive disorder. *Clinical Neurophysiology*.

Lee, J. Y., Mucksavage, P., Sundaram, C. P., and McDougall, E. M. (2011). Best practices for robotic surgery training and credentialing. *The Journal of urology*, **185**(4), 1191–1197.

Li, K. W. (2002). Ergonomic design and evaluation of wire-tying hand tools. *International Journal of Industrial Ergonomics*, **30**(3), 149–161.

Mason, J. D., Ansell, J., Warren, N., and Torkington, J. (2012). Is motion analysis a valid tool for assessing laparoscopic skill? *Surgical endoscopy*, pages 1–10.

Matern, U. and Waller, P. (1999). Instruments for minimally invasive surgery. *Surgical endoscopy*, **13**(2), 174–182.

McDougall, E. M. and ClayMan, R. V. (1996). *Laparoscopic nephrectomy for benign disease: comparison of the transperitoneal and retroperitoneal approaches*, volume 10.

Mercier, L., Langø, T., Lindseth, F., and Collins, L. D. (2005). A review of calibration techniques for freehand 3-d ultrasound systems. *Ultrasound in medicine & biology*, **31**(2), 143–165.

Moorthy, K., Munz, Y., Sarker, S. K., and Darzi, A. (2003). Objective assessment of technical skills in surgery. *BMJ: British Medical Journal*, **327**(7422), 1032.

Reznick, R., Regehr, G., MacRae, H., Martin, J., and McCulloch, W. (1997). Testing technical skill via an innovative bench station examination. *The American Journal of Surgery*, **173**(3), 226–230.

Riener, R., Reiter, S., Rasmus, M., Wetzel, D., and Feussner, H. (2003). Acquisition of arm and instrument movements during laparoscopic interventions. *Minimally Invasive Therapy & Allied Technologies*, **12**(5), 235–240.

Ropella, K. M. (2007). *Introduction to statistics for biomedical engineers*, volume 2. Morgan & Claypool Publishers.

Schoonjans, F., De Bacquer, D., and Schmid, P. (2011). Estimation of population percentiles. *Epidemiology*, **22**(5), 750–751.

Segre, A. M. (1992). *Applications of machine learning*, volume 7.

Sidhu, R., Grober, E., Musselman, L., and Reznick, R. (2004). Assessing competency in surgery: where to begin? *Surgery*, **135**(1), 6–20.

Statnikov, A., Hardin, D., Guyon, I., and Aliferis, C. F. (2011). *A Gentle Introduction to Support Vector Machines in Biomedicine*. World Scientific.

Stylopoulos, N. and Vosburgh, K. G. (2007). Assessing technical skill in surgery and endoscopy: A set of metrics and an algorithm (c-pass) to assess skills in surgical and endoscopic procedures. *Surgical Innovation*, **14**(2), 113–121.

Tausch, T. J., Kowalewski, T. M., White, L. W., McDonough, P. S., Brand, T. C., and Lendvay, T. S. (2012). Content and construct validation of a robotic surgery curriculum using an electromagnetic instrument tracker. *The Journal of urology*.

Theodoridis, S. (2003). *Pattern Recognition*. Academic Press.

trakStar (2009). *3D Guidance trakSTAR manual*.

Van Sickle, K., McClusky III, D., Gallagher, A., and Smith, C. (2005). Construct validation of the promis simulator using a novel laparoscopic suturing task. *Surgical Endoscopy and Other Interventional Techniques*, **19**(9), 1227–1231.

Wang, S. and Summers, R. M. (2012). Machine learning and radiology. *Medical image analysis*, **16**(5), 933–951.

Xeroulis, G., Dubrowski, A., and Leslie, K. (2009). Simulation in laparoscopic surgery: a concurrent validity study for fls. *Surgical endoscopy*, **23**(1), 161–165.

Zhou, J., Sebastian, E., Mangona, V., and Yan, D. (2013). Real-time catheter tracking for high-dose-rate prostate brachytherapy using an electromagnetic 3d-guidance device: A preliminary performance study. *Medical physics*, **40**, 021716.